NUMERICAL STUDIES ON THE KLEIN-GORDON-SCHRÖDINGER EQUATIONS IN THE SINGULAR LIMIT REGIME

HONG MEI

NATIONAL UNIVERSITY OF SINGAPORE

2015

NUMERICAL STUDIES ON THE KLEIN-GORDON-SCHRÖDINGER EQUATIONS IN THE SINGULAR LIMIT REGIME

HONG MEI

(B.Sc., Xi'an Jiaotong University, China)

A THESIS SUBMITTED

FOR THE DEGREE OF MASTER OF SCIENCE

DEPARTMENT OF MATHEMATICS

NATIONAL UNIVERSITY OF SINGAPORE

2015

Declaration

I hereby declare that the thesis is my original work and it has been written by me in its entirety. I have duly acknowledged all the sources of information which have been used in the thesis.

This thesis has also not been submitted for any degree in any university previously.

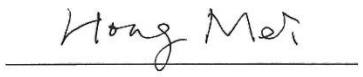

Hong Mei

August 12, 2015

Acknowledgements

It is my great honor to take this opportunity to thank those who made this thesis possible.

First and foremost, I owe my deepest gratitude to my supervisor Prof. Bao Weizhu, whose generous support, patient guidance, constructive suggestion, invaluable help and encouragement enabled me to conduct such an interesting research project. His patience, his wise wisdom and his attitude towards research work gave great impression and had great influence on me.

It is also my pleasure to express my appreciation and gratitude to Zhao Xiaofei and Ruan Xinran, from whom I got valuable suggestions and great help on my research project. My sincere thanks go to all the former colleagues and fellow graduates in our group. My heartfelt thanks go to my friends for all the encouragement, emotional support, comradeship and entertainment they offered. I would also like to thank NUS for awarding me the Research Scholarship during the period of my MSc candidature and my sincere thanks go to the Mathematics Department of NUS for its kind help during my two-years study.

Last but not least, I am forever indebted to my beloved boy friend and family, for their encouragement, steadfast support and endless love when it was most needed.

Hong Mei

August 2015

Contents

Summary

Klein-Gordon-Schrödinger (KGS) equations describes a system of a conserved scalar nucleon interacting with a neutral scalar meson coupled through the Yukawa interaction. It has a wide range of applications, including but not limited to the study of the dynamics of small but finite amplitude nonlinearly interacting perturbations in many-body physics, nonlinear optics and optical communications, nonlinear plasmas and complex geophysical flows, as well as the intense laser-plasma interactions.

The purpose of this thesis is to propose and analyze efficient and uniformly accurate numerical methods for solving the KGS equations in the singular limit regime, i.e., $0 < \varepsilon \ll 1$. We propose two exponential wave integrator methods and two multiscale methods. Before the analysis of these methods, we apply some existing numerical methods for solving the KGS equations in the singular limit regime to acknowledge their limitations. In order to understand how the step size should be chosen when ε is very small, we pay special attention to studying the error bound of each method.

This thesis mainly contains two parts. In the first part, some accurate and efficient methods, such as energy conservative finite difference (ECFD) method, semi-implicit finite difference (SIFD) method and Crank-Nicolson time-splitting Fourier

pseudospectral (CNTSFP) method, are proposed and analyzed for solving the KGS equations with periodic boundary conditions and three types of initial data, i.e., the well-prepared, the ill-prepared and the extremely ill-prepared initial data. The error estimate of ECFD when $\varepsilon = O(1)$ is provided, which shows the error bound and convergence rate of the ECFD from theoretical point of view. Extensive numerical results on the KGS equations with the three types of initial data are reported to demonstrate the efficiency, accuracy and ε-scalability. Based on the numerical results, we find that all the methods have uniform accuracy in space for solving the KGS equations with different types of initial data except for the ECFD and SIFD methods, which show $h^2/\sqrt{\varepsilon}$ error bound in space for solving the extremely ill-prepared data problem. All the methods have uniform second-order accuracy in time only for solving the KGS equations with the well-prepared initial data when $0 < \varepsilon \ll 1$. The numerical results also show that ECFD, SIFD and CNTSFP have asymptotic temporal error bound $O(k^2/\varepsilon^2)$ for solving the ill-prepared initial data problem and $O(k^2/\varepsilon^3)$ for solving the extremely ill-prepared initial data problem. In addition, all of the methods have some convergence order reductions or lose the convergence of temporal error outside the convergence regime, which means that when ε is very small, these methods are not efficient nor optimal for solving the KGS equations numerically except for taking k sufficiently small.

The second part tackles the KGS equations with the ill-prepared initial and the extremely ill-prepared initial data in the singular limit regime, of which the solutions have high oscillation in time with respect to ε. Based on the exponential wave integrator (EWI) method for solving the second order nonlinear ODEs and time-splitting algorithm for the Schrödinger equation, we propose two uniformly accurate, efficient and explicit methods. The two exponential wave integrator time-splitting Fourier pseudospectral (EWI-TSFP) methods are designed by using a pseudospectral method for spatial derivatives of the Kelin-Gordon equation, and then using the Gautschi-type exponential wave integrator method for solving the second-order ODEs, and coupling with the time-splitting Fourier pseudospectral method for the

NLSE. Numerical studies of these two methods are carried out for the ill-prepared and extremely ill-prepared problem, which show that these two methods have uniform and optimal spectral accuracy in space. Moreover, the two methods are uniformly accurate in time and optimally convergent with quadratic rate when $0 < k \leq \varepsilon$. Compared with the results of the classical methods, the new methods offer better approximations for the KGS equations when $0 < \varepsilon \ll 1$. And the new methods can be easily extended to 2D and 3D problems and are easy to implement. Finally, we propose the multiscale analysis of the KGS equations to know the main properties of the solutions to the KGS equations theoretically under the three main types of initial conditions. Two multiscale methods are proposed with the application of the two EWI-TSFP methods to the decomposed KGS equations with ill-prepared initial data. Numerical results show that the multiscale methods have uniform spectral accuracy in space and uniform second-order accuracy in time. Thus for solving the KGS equations with ill-prepared initial data, the multiscale methods are the best with uniform and optimal accuracy compared with the other methods we discussed.

List of Tables

List of Figures

List of Symbols and Abbreviations

t	time
τ	fast time scale
$\mathbf{x}$	Cartesian coordinate
$\mathbb{R}^d$	d dimensional Euclidean space
$\mathbb{C}^d$	d dimensional complex space
k	time step size
h	space mesh size
i	imaginary unit
ε	a dimensionless parameter with its value $0 < \varepsilon \leq 1$
∇	gradient
$\Delta = \nabla \cdot \nabla$	Laplacian
$\bar{f}$	conjugate of of a complex function f
$\hat{f}$	Fourier transform of function f
$\widetilde{f}$	discrete Fourier transform of a vector f
$\mathrm{Re}(f)$	real part of a complex function f
$\mathrm{Im}(f)$	imaginary part of a complex function f
$A \lesssim B$	$A \leq C \cdot B$ for some positive constant C independent of $k,\ h$ and ε

1D	one dimension
2D	two dimension
3D	three dimension
$\|\cdot\|_{H^m(\mathbb{R}^d)}$	the norm in the Hilbert space
KGS	Klein-Gordon Schrödinger
SY	Schrödinger-Yukawa
NLSE	Nonlinear Schrödinger equation
BC	boundary condition
ECFD	Energy conservative finite difference
SIFD	Semi-implicit finite difference
CNTSFP	time-splitting Crank-Nicolson Fourier pseudospectral
EWI-TSFP	Exponential wave integrator and time-splitting Fourier pseudospectral method
EWI-TSFP2	Another exponential wave integrator and time-splitting pseudospectral method
MEWI-TSFP	Multiscale EWI-TSFP
MEWI-TSFP2	Multiscale EWI-TSFP2
Fig.	Figure
Tab.	Table
Figs.	Figures
Tabs.	Tables

Chapter 1

Introduction

1.1 Physical background

During the past decades, a wide range of physical phenomena are explained by the dynamics of nonlinear waves [15]. One of the most challenging and modern applications of the control of the nonlinear waves is the control of quantum-mechanical systems [17, 20, 33, 53, 65, 68, 86]. It has become clear that the same equations, such as the nonlinear Schrödinger (NLS) equation, the Sine-Gordon equation and Klein-Gordon equation etc., appear in many different physical situations (see, for example, [66, 72] and the references therein). It makes sense to introduce some efficient methods for solving the same equations with different restrictive conditions. Furthermore, for the nonlinear waves describing the phenomena in quantum and plasma physics, oscillations could occur either in space or in time or in both. For example, the nonlinear Schrödinger equation in the semiclassical limit regime has oscillations in both time and space [12], the nonlinear Klein-Gorden equation in the nonrelativistic limit regime [8] is highly oscillatory in time and so are the Klein-Gordon-Zarharov system [9] and Zarkharov system [13] in the subsonic limit regime. Uniformly accurate methods are needed to solve those oscillation problems. Much research has been done during these two decades. For our interest, we will focus on the Klein-Gordon-Schrödinger (KGS) equations (system) in the singular limit

regime to find the effective approximations of the system with different kinds of initial conditions, getting rid of the influence of the oscillation.

As we know, the standard Klein-Gordon-Schrödinger-Yukawa system describes a classical model of the Yukawa interaction between conservative complex nucleon field and neutral meson in quantum field theory [91]. The KGS system has wide application in many physical fields (see [69, 73, 79] and the references therein). For example, a similar system to these equations may describe the dynamics of coupled high frequency electron waves and low frequency ion plasma waves in a homogeneous magnetic field [30]. In addition, the KGS equations have been widely used to study the dynamics of small but finite amplitude nonlinearly interacting perturbations in many-body physics [30], nonlinear optics and optical communications [71], nonlinear plasmas and complex geophysical flows [43], as well as the intense laser-plasma interactions [72] and nonlinear quantum electrodynamics [66]. As is well known, many researchers have been working on the solutions for the classical KGS equations theoretically and numerically and most of them focused on the classical KGS equations with particular kind of initial data or boundary condition. Here, the numerical studies for the KGS equations in the singular limit regime are essential and necessary.

1.2 The Klein-Gordon-Schrödinger equations

The nonlinear Schrödinger equation coupled with a nonlinear Klein-Gordon equation reads

$$i\partial_t\psi(\mathbf{x},t)+\Delta\psi(\mathbf{x},t)+\psi(\mathbf{x},t)\phi(\mathbf{x},t)=0,\mathbf{x}\in\mathbb{R}^d,\ t>0, \tag{1.1}$$

$$\varepsilon^2\partial_{tt}\phi(\mathbf{x},t)-\Delta\phi(\mathbf{x},t)+\beta\phi(\mathbf{x},t)-|\psi(\mathbf{x},t)|^2=0,\ \mathbf{x}\in\mathbb{R}^d,t>0, \tag{1.2}$$

with the initial conditions

$$\psi(\mathbf{x},0)=\psi^{(0)}(\mathbf{x}),\ \phi(\mathbf{x},0)=\phi^{(0)}(\mathbf{x}),\ \partial_t\phi(\mathbf{x},0)=\phi^{(1)}(\mathbf{x}),\ \mathbf{x}\in\mathbb{R}^d. \tag{1.3}$$

The system of Eqs. (1.1) and (1.2), which is known as the Klein-Gorden-Schrödinger equations, is a classical example describing a system of a conserved scalar nucleon interacting with a neutral scalar meson coupled though the Yukawa interaction [91]. Here, the complex-valued unknown function $\psi(\mathbf{x},t)$ represents a scalar nucleon field, the real-valued unknown function $\phi(\mathbf{x},t)$ represents a scalar meson field, $\varepsilon>0$ is a parameter inversely proportional to the speed of light, β is one nonnegative constant. In fact, when $\varepsilon=1$ and $\beta=1$, the system (1.1)-(1.2) reduces to the standard KGS equations [34]. When $0<\varepsilon\ll 1$ and $\beta=O(1)$, the system (1.1)-(1.2) is called the KGS equations in the singular limit regime. Here throughout this thesis we assume that $\beta=1$. It is easy to see that the KGS equations have the following two important conserved quantities, i.e. the wave energy

$$D(t):=\int_{\mathbb{R}^d}|\psi(\mathbf{x},t)|^2d\mathbf{x}=\int_{\mathbb{R}^d}|\psi^{(0)}(\mathbf{x})|^2d\mathbf{x}\equiv D(0),\ t\geq 0. \tag{1.4}$$

and the Hamiltonian

$$\begin{aligned}H(t)=\int_{\mathbb{R}^d}\bigg[&\frac{1}{2}(\phi(\mathbf{x},t)^2+\varepsilon^2(\partial_t\phi(\mathbf{x},t))^2+(\nabla\phi(\mathbf{x},t))^2)+|\nabla\psi(\mathbf{x},t)|^2\\&-|\psi(\mathbf{x},t)|^2\phi(\mathbf{x},t)\bigg]d\mathbf{x}\equiv H(0),\ t\geq 0.\end{aligned} \tag{1.5}$$

In the singular limit regime, i.e. $\varepsilon\to 0$, the KGS equations collapse to the nonlinear Schrödinger-Yukawa (SY) equations:

$$i\partial_t\psi^0(\mathbf{x},t)+\Delta\psi^0(\mathbf{x},t)+\phi^0(\mathbf{x},t)\psi^0(\mathbf{x},t)=0, \tag{1.6}$$

$$-\Delta\phi^0(\mathbf{x},t)+\phi^0(\mathbf{x},t)-|\psi^0(\mathbf{x},t)|^2=0,\ \mathbf{x}\in\mathbb{R}^d,\ t\geq 0, \tag{1.7}$$

with the initial condition

$$\psi^0(\mathbf{x},0):=\psi_l^0(\mathbf{x})=\lim_{\varepsilon\to 0}\psi^{(0)}(\mathbf{x}),\quad x\in\mathbb{R}^d, \tag{1.8}$$

where $\psi^0(\mathbf{x},t)=\lim\limits_{\varepsilon\to 0}\psi(\mathbf{x},t)$ and $\phi^0(\mathbf{x},t)=\lim\limits_{\varepsilon\to 0}\phi(\mathbf{x},t)$. In addition, when $t=0$, the solutions of the SY equations satisfy [10]

$$\phi_l^0(\mathbf{x}):=\phi^0(\mathbf{x},0)=(-\Delta+I)^{-1}|\psi_l^0|^2, \tag{1.9}$$

$$\phi_l^1(\mathbf{x}):=\partial_t\phi^0(\mathbf{x},0)=-i(-\Delta+I)^{-1}\nabla\cdot(\psi_l^0\nabla\bar{\psi}_l^0-\bar{\psi}_l^0\nabla\psi_l^0). \tag{1.10}$$

The corresponding conservation laws hold for the SY equations with the Hamiltonian

$$H^0(t) = \int_{\mathbb{R}^d} \Big[\frac{1}{2}(\phi^0(\mathbf{x},t)^2 + (\nabla\phi^0(\mathbf{x},t))^2) + |\nabla\psi^0(\mathbf{x},t)|^2 \\ - |\psi^0(\mathbf{x},t)|^2\phi^0(\mathbf{x},t) \Big] d\mathbf{x} \equiv H(0),\ t \geq 0. \tag{1.11}$$

Here the initial data in (1.3) can be classified into the three types with $m \geq 2$ as follows:

(i) Well-prepared initial data; i.e., there exists one constant ε_1 such that for $0 < \varepsilon \leq \varepsilon_1$,

$$\|\psi^{(0)} - \psi_l^0\|_{H^m(\mathbb{R}^d)} + \|\phi^{(0)} - \phi_l^0\|_{H^m(\mathbb{R}^d)} + \|\varepsilon(\phi^{(1)} - \phi_l^1)\|_{H^m(\mathbb{R}^d)} \lesssim \varepsilon^2. \tag{1.12}$$

(ii) Ill-prepared initial data; i.e., there exists one constant ε_2 such that for $0 < \varepsilon \leq \varepsilon_2$,

$$\|\psi^{(0)} - \psi_l^0\|_{H^m(\mathbb{R}^d)} + \|\phi^{(0)} - \phi_l^0\|_{H^m(\mathbb{R}^d)} + \|\varepsilon(\phi^{(1)} - \phi_l^1)\|_{H^m(\mathbb{R}^d)} \lesssim \varepsilon. \tag{1.13}$$

(iii) Extremely ill-prepared initial data; i.e., there exists one constant ε_2 such that for $0 < \varepsilon \leq \varepsilon_2$,

$$\|\psi^{(0)} - \psi_l^0\|_{H^m(\mathbb{R}^d)} \lesssim \varepsilon,\ \|\phi^{(0)} - \phi_l^0\|_{H^m(\mathbb{R}^d)} + \|\varepsilon(\phi^{(1)} - \phi_l^1)\|_{H^m(\mathbb{R}^d)} = O(1). \tag{1.14}$$

In our studies on the KGS equations in the singular limit regime, we will test our numerical results of each method with these initial data respectively.

1.3 Contemporary studies

The KGS equations in the classical regime, i.e., $\varepsilon = O(1)$, has been studied for several decades. There are mainly two aspects of their research. One is developed from the pure mathematics and physics in which the methods are known as the analytical studies in the literature. The other is from the computational mathematics and physics studies where people developed different numerical methods for

the KGS equations. On the analytical studies, the first study was done by Fukuda and Tsutsumi [34]- [36]. By using the Galerkin's method, they proved the unique existence of global strong solutions of the initial boundary value problem. Baillon and Chadam [2] proved the existence of global strong solutions of the initial value problem of the KGS equations by using $L^p - L^q$ estimates for the elementary solution of the linear Schrödinger equation. Hayashi and Wahl [44] did some extension and showed the existence of global strong solutions to the initial boundary value problem by using estimates of the nonlinearity in fractional order Besov space developed by Brenner and Wahl [18], nonlinear interpolation theorem obtained by Whal [75]- [77], the inequality of Brezis and Gallouet [19]. Ozawa and Tsutsumi [63] studied the asymptotic behavior of solutions for the KGS equations. Later, Guo and Miao [40] studied asymptotic states; Li and Guo [57] studied the asymptotic smoothing effect of solutions to weakly dissipative KGS equations. Ohta [62] established the stability of stationary states and Natali [61] found the stability properties of the periodic standing waves. Biler [16] studied the attractors of the system and also gave some estimates on the decay of the homogeneous dissipative system. Lu and Wang [59], Guo and Li [41] found the global attractors. The solitary wave solutions to Eqs. (1.1) and (1.2) have been obtained by using the homogeneous balance method [84]. And Zhou and Wang [78] found the periodic wave solutions expressed by various Jacobi elliptic functions of (1.1) and (1.2) by using F-expansion method which can be thought of as a generalization of Jacobi elliptic function expansion method. Hioe [47] has obtained the periodic solitary waves for the two coupled nonlinear KGS equations. Fan et al. [24] have proposed an algebraic method to obtain the explicit exact solutions for coupled KGS equations. Yomba [90] applied the mapping method to construct the explicit, rich and new solutions such as Jacobi elliptic function, combined Jacobi elliptic function, rational, triangular function, soliton and combined soliton solutions. Recently, Hesameddini and Fotros [45] found the solution for the time-fractional coupled KGS equation by using decomposition method. In addition, more reference about the plane, global and solitary wave solutions of the standard

KGS equations, we refer to [1, 24, 28, 39, 51, 84, 88] and the reference therein.

Study with regard to numerical approximation is a hot topic for this problem recently since the numerical methods are important tools for understanding the physical behavior of the equations. Zhang [93] studied a conservative finite difference method (C-C) for the standard KGS and provided the detailed error estimates by energy method. Kong et al. [55] paid attention to its structure-preserving numerical schemes and experimentally discussed it. Then they derived multisymplectic midpoint (M-M) scheme. In [54], they also presented the symplecticity for the KGS and proposed a symplectic structure-preserving integrator for it. However, the methods are completely implicit and tedious iterative process is required. Hong [50] proposed three finite difference schemes, which are called M-C, T-C and T-T schemes and compared the numerical behavior of the three schemes with those of the schemes C-C and M-M in the same paper. These finite difference schemes applied to the KGS equations are implicit and requires huge computation cost for initial or initial-boundary value problems. Wang and Zhang [80] derived a class of discrete-time orthogonal spline collocation schemes. Xanthopoul and Zouraris [87] investigated the KGS equations by using a linearly implicit method. Hong et al. [49] proposed the explicit multi-symplectic schemes by concatenating suitable symplectic Runge-Kutta-type methods and symplectic Runge-Kutta-Nyström-type methods for discretizing every partial derivative in each sub-equation. Wang [82] gave the optimal point-wise error estimate of a compact difference scheme. In [67], the modified decomposition method was also proposed to solve the KGS equations.

Due to the high accuracy, spectral methods have been increasingly popular during these two decades. Kong et al. [56] proposed an explicit symplectic partitioned Runge-Kutta Fourier pseudospectral scheme for the KGS equations. They also presented the symplecticity for the KGS equations and proposed a symplectic structure-preserving integrator for it. Xiang [89] proposed a conservative spectral method with

the periodic initial conditions. Bao and Yang [14] suggested two time-splitting pseudospectral methods. In one method, they used Fourier pseudospectral discretization for the spatial derivatives and Crank-Nicolson/Leap-Frog schemes for the time derivatives including time splitting methods for the Schrödinger equation. For another one, they used Fourier pseudospectral discretization for the spatial derivatives and then solved the ODEs in phase analytically. Cai et al. [21] proposed explicit and implicit multisymplectic Fourier pseudospectral schemes for the equations. Dehghan and Taleei [29] investigated the KGS equations by using Chebyshev pseudospectral collocation method for the approximation in the spatial variable and the explicit Runge-Kutta method in time discretization for the KGS equations. Very recently, Liang [58] designed a linearly implicit conservative scheme for long-term numerical simulation of the KGS equations, which is new charge-preserving and energy-preserving Fourier pseudospectral algorithm for the KGS equations.

On the other hand, for the KGS equations (1.1) and (1.2) in the singular limit regime, i.e., $0 < \varepsilon \ll 1$, very few analytical and numerical results are available in the literature. Only Bao and Yang [14] contributed the time-splitting pseudospectral methods and studied ε-resolution of the KGS equations with well-prepared initial data or solitary initial data. And in [10], Bao et al. provided rigorous mathematical justification for the formal limits of the solution of the KGS equations to the solution of the SY equation based on the two-scale matched asymptotic expansion. Thus, more attentions are needed to analyze the solutions and to design efficient and accurate numerical methods of (1.1)-(1.2) in the singular limit regime. In fact, due to the two-scale matches asymptotic analysis, there are high oscillations in the solutions of the KGS equations with the ill-prepared or extremely ill-prepared initial data when $\varepsilon \to 0$. This brings some difficulties in the mathematical analysis and causes severe burdens in practical computation of the KGS equations in the singular limit regime, making the analytical and numerical approximations extremely challenging and costly in the regime of $0 < \varepsilon \ll 1$. However, some uniformly accurate numerical schemes for highly oscillatory Klein-Gordon equation and the nonlinear Schrödinger

equation have been proposed and analyzed in [7, 22] recently. The method in [22] is based on embedding the problem in a suitable two-scale reformulation by introducing an additional variable and using the Chapman-Enskog expansion to separate the fast time scale and the slow one, while this method increases the dimension of the problem. And the method in [7] is designed by adapting a multiscale decomposition by frequency (MDF) to the solution at each time step and applying an exponential wave integrator [37, 38] to the nonlinear Schrödinger equation with wave operators. Therefore, it is desirable and hopeful to design simple and efficient, as well as easy to implement, uniformly accurate numerical methods for the KGS equations when $\varepsilon \in (0, 1]$ with balance between efficiency and accuracy as well as simplicity.

1.4 Purpose and scope of this thesis

The purpose of this study is to propose and analyze efficient and accurate numerical methods for solving the Klein-Gordon-Schrödinger equations in the singular limit regime. We mainly focus on the following two parts:

- Firstly, to present some existing numerical methods for discretizing the KGS equations on bounded domains under different initial data to understand numerically how the initial conditions influence the solutions. Meanwhile, we study ε-scalability of different classical numerical methods and detailed comparison of these methods is made.

- Secondly, to propose some simple, uniformly accurate and efficient numerical methods to solve the KGS equations in the singular limit regime.

The following chapters are organized as follows. Chapter 2 is devoted to studying some existing numerical methods to the KGS equations with different initial data and detailed comparison is provided in the last part of this chapter. We paid particular attention to the resolution of different numerical methods, i.e., meshing strategy requirement (or ε-scalability) for solving the KGS equations with different initial

data when $0 < \varepsilon \ll 1$. In Chapter 3, we applied the exponential wave integrator (EWI) with the Gautschi's quadratue Fourier pseudospectral method to the Klein-Gordon equation in the KGS system, and coupled with time-splitting method for the Schrödinger equation to obtain two uniformly accurate schemes for the KGS equations in the singular limit regime with different initial conditions. The methods are explicit, efficient, and accurate in practical computation and converge optimally at quadratic convergence rate in the regimes $\varepsilon = O(1)$. Thus the methods in Chapter 3 are very different from those methods in Chapter 2. In fact, similar techniques were already used for discretizing the Zakharov system [13]. In Chapter 4, we proposed the multiscale analysis of the KGS equations in order to know the main properties of the solutions to the KGS equations theoretically under three main types of initial conditions. Two multiscale methods were proposed with the application of the two EWI-TSFP methods for the decomposed KGS equations under the ill-prepared initial conditions. In Chapter 5, we got some conclusions and discussed some possible future work.

Chapter 2

Standard numerical methods and their analysis

In this chapter, we are going to apply and study some popular classical numerical methods which are proposed based on directly discretizing the classical KGS equations. Special efforts are made to study how the error bound of the numerical method depends on ε, as $0 < \varepsilon \ll 1$. Zhang [93] has proposed an energy conservative finite difference method to solve the KGS equations with $\varepsilon = 1$. A detailed review and application of this method and a semi-implicit finite difference method for the KGS equations in the singular limit regime are provided in section 2.1. We also provide the detailed proof of error estimate when $\varepsilon = O(1)$. In section 2.2, we briefly review one time-splitting method, which is Crank-Nicolson Fourier pseudospectral discretization, coupled with time-splitting Fourier pseudospectral (TSFP) method for the NLSE. Extensive numerical results on the three types of initial problems are reported to demonstrate the efficiency, accuracy and ε-scalability of these methods in Section 2.3.

2.1 Finite difference methods and their analysis

In this section, we present some numerical methods for the KGS equations with periodic boundary conditions. For simplicity of notation, we shall introduce the method in one space dimension ($d = 1$). Generalizations to $d > 1$ are straightforward for the tensor product grids, and the results remain valid without modifications. In one dimension, the problem collapses to

$$i\partial_t\psi + \Delta\psi + \phi\psi = 0,\ a < x < b,\ t > 0, \tag{2.1}$$

$$\varepsilon^2\partial_{tt}\phi - \Delta\phi + \phi - |\psi|^2 = 0,\ a < x < b,\ t > 0, \tag{2.2}$$

$$\psi(x,0) = \psi^{(0)}(x),\ \phi(x,0) = \phi^{(0)}(x),\ \partial_t\phi(x,0) = \phi^{(1)}(x),\ a \le x \le b, \tag{2.3}$$

$$\psi(a,t) = \psi(b,t),\ \partial_x\psi(a,t) = \partial_x\psi(b,t),\ t \ge 0, \tag{2.4}$$

$$\phi(a,t) = \phi(b,t),\ \partial_x\phi(a,t) = \partial_x\phi(b,t),\ t \ge 0. \tag{2.5}$$

Moreover, we supplement (2.1-2.5) by imposing the compatibility condition

$$\psi^{(0)}(a) = \psi^{(0)}(b),\ \phi^{(0)}(a) = \phi^{(0)}(b),\ \phi^{(1)}(a) = \phi^{(1)}(b). \tag{2.6}$$

We remark here that the boundary conditions considered here are inspired by the inherent physical nature and they have been widely used in the literature for dealing with analysis and computation of the KGS equations. As is well known, the above KGS equations in 1D have the following properties:

$$D(t) = \int_a^b |\psi(x,t)|^2 dx = \int_a^b |\psi^{(0)}(x)|^2 dx = D(0),\ t \ge 0, \tag{2.7}$$

and the Hamiltonian

$$\begin{aligned} H(t) = \int_a^b \Big[&\frac{1}{2}(\phi(x,t)^2 + \varepsilon^2(\partial_t\phi(x,t))^2 + (\partial_x\phi(x,t))^2) + |\partial_x\psi(x,t)|^2 \\ &- |\psi(x,t)|^2\phi(x,t)\Big] dx = H(0),\ t \ge 0. \end{aligned} \tag{2.8}$$

In some cases, the periodic boundary conditions (2.4) and (2.5) may be replaced by the homogeneous Dirichlet boundary conditions, i.e.,

$$\psi(a,t) = \psi(b,t) = 0,\ \phi(a,t) = \phi(b,t) = 0,\ t \ge 0. \tag{2.9}$$

We choose the spatial mesh size $h = \Delta x > 0$ with $h = (b-a)/M$ for M an even positive integer, the time step $k = \Delta t > 0$, and let the grid points and the time step be $x_j := a + jh,\ j = 0, 1, \cdots M,\ t_n := nk,\ n = 0, 1, \cdots$. Let ψ_j^n and ϕ_j^n be the approximations of $\psi(x_j, t_n)$ and $\phi(x_j, t_n)$ $(j = 0, 1, \cdots M\ n = 0, 1, \cdots)$ and introduce the finite difference discretization operator as following, for $u^n = (u_0, u_1, u_2, \cdots u_M)$

$$(u_j^n)_x = \frac{u_{j+1}^n - u_j^n}{h}, \quad (u_j^n)_{\bar{x}} = \frac{u_j^n - u_{j-1}^n}{h},$$

$$(u_j^n)_t = \frac{u_j^{n+1} - u_j^n}{k}, \quad (u_j^n)_{\bar{t}} = \frac{u_j^n - u_j^{n-1}}{h},$$

$$(u_j^n)_{\hat{t}} = \frac{u_j^{n+1} - u_j^{n-1}}{2k}, \quad \|u^n\|_\infty = \sup_{1\le j\le M} |u_j^n|,$$

$$(u^n, v^n) = h\sum_{j=0}^{M-1} u_j^n \bar{v}_j^n, \ \|u^n\|_p^p = h\sum_{j=0}^{M-1} |u_j^n|^p,$$

$$\|u^n\|_{H^1} = \sqrt{h\sum_{j=0}^{M-1} |u_j^n|^2} + \sqrt{h\sum_{j=0}^{M-1} |\frac{u_{j+1}^n - u_j^n}{h}|^2}.$$

Then the energy conservative finite difference (ECFD) method reads:

$$i\frac{\psi_j^{n+1} - \psi_j^n}{k} + \frac{1}{2}(\psi_j^{n+1} + \psi_j^n)_{x\bar{x}} + \frac{1}{4}(\psi_j^{n+1} + \psi_j^n)(\phi_j^{n+1} + \phi_j^n) = 0, \tag{2.10}$$
$$0 \le j \le M-1,\ n \ge 0,$$

$$\varepsilon^2(\phi_j^n)_{t\bar{t}} - \frac{1}{2}(\phi_j^{n+1} + \phi_j^{n-1})_{x\bar{x}} + \frac{1}{2}(\phi_j^{n+1} + \phi_j^{n-1}) - |\psi_j^n|^2 = 0, \tag{2.11}$$
$$0 \le j \le M-1,\ n \ge 1,$$

$$\psi_0^n = \psi_M^n,\ \phi_0^n = \phi_M^n,\ \psi_{-1}^n = \psi_{M-1}^n,\ \phi_{-1}^n = \phi_{M-1}^n,\ n \ge 0. \tag{2.12}$$

The initial conditions (2.3) are discretized as

$$\psi_j^0 = \psi^{(0)}(x_j),\ \phi_j^0 = \phi^{(0)}(x_j), \quad j = 0, 1, \cdots M, \tag{2.13}$$

$$\phi_j^1 = \phi_j^0 + k\phi^{(1)}(x_j) + \frac{k^2}{2\varepsilon^2}\left((\Delta\phi^{(0)})(x_j) - \phi_j^0 + |\psi_j^0|^2\right),\ j = 0, 1, \cdots M. \tag{2.14}$$

And a semi-implicit finite difference (SIFD) method reads

$$\begin{aligned} &i\frac{\psi_j^{n+1}-\psi_j^{n-1}}{2k}+\frac{1}{2}(\psi_j^{n+1}+\psi_j^{n-1})_{x\bar{x}}+(\psi_j^n\phi_j^n)=0,\\ &0\le j\le M-1,\ n\ge 0, \end{aligned} \tag{2.15}$$

$$\begin{aligned} &\varepsilon^2(\phi_j^n)_{t\bar{t}}-\frac{1}{2}(\phi_j^{n+1}+\phi_j^{n-1})_{x\bar{x}}+\frac{1}{2}(\phi_j^{n+1}+\phi_j^{n-1})-|\psi_j^n|^2=0,\\ &0\le j\le M-1,\ n\ge 1, \end{aligned} \tag{2.16}$$

$$\psi_0^n=\psi_M^n,\ \phi_0^n=\phi_M^n,\ \psi_{-1}^n=\psi_{M-1}^n,\ \phi_{-1}^n=\phi_{M-1}^n,\ n\ge 0. \tag{2.17}$$

And the initial data are the same with those of ECFD. This scheme is easier to compute than ECFD but does not conserve energy of the KGS equations in the discrete level.

2.1.1 Energy conservation laws

For the ECFD method, one can easily show that the scheme satisfies the following conservation laws in discrete level. We can assume that the solutions of the KGS equations satisfy

$$\begin{aligned} &\phi(x,t)\in(C^4[a,b];W^{1,\infty})\cap(C^3[a,b];W^{2,\infty})\cap(C^2[a,b];W^{3,\infty})\cap C[a,b],\\ &\psi(x,t)\in(C^3[a,b];W^{1,\infty})\cap(C^2[a,b];W^{2\infty})\cap C[a,b]. \end{aligned} \tag{A}$$

Lemma 2.1.1. *The ECFD scheme satisfies the following two conservation laws:*

$$\mathcal{E}^n=\mathcal{E}^{n-1}=\cdots=\mathcal{E}^0, \tag{2.18}$$

$$\|\psi^{n+1}\|_2^2=\|\psi^n\|_2^2=\cdots\|\psi^0\|_2^2, \tag{2.19}$$

where

$$\begin{aligned} \mathcal{E}^n=&\varepsilon^2\|\phi_t^n\|_2^2+\frac{1}{2}(\|\phi_x^n\|_2^2+\|\phi_x^{n+1}\|^2)+\frac{1}{2}(\|\phi^n\|_2^2+\|\phi^{n+1}\|^2)\\ &+2\|\psi_x^{n+1}\|_2^2-h\sum_{j=1}^{M-1}(\phi_j^n+\phi_j^{n+1})|\psi_j^{n+1}|^2. \end{aligned} \tag{2.20}$$

Proof. Computing the product of discrete KG equation (2.10) with $h(\bar{\psi}_j^{n+1} + \bar{\psi}_j^n)$, summing up with j and taking the imaginary part, we obtain

$$\frac{1}{k}(\|\psi^{n+1}\|_2^2 - \|\psi^n\|_2^2) = 0. \tag{2.21}$$

Thus

$$\|\psi^{n+1}\|_2^2 = \|\psi^n\|_2^2 = \cdots \|\psi^0\|_2^2. \tag{2.22}$$

Computing the product of discrete KG equation (2.10) with $h(\bar{\psi}_j^{n+1} - \bar{\psi}_j^n)$, summing up with j and taking the real part, we get

$$\|\psi_x^{n+1}\|_2^2 - \|\psi_x^n\|_2^2 - \frac{1}{2}h\sum_{j=1}^{M-1}(\phi_j^{n+1} + \phi_j^n)(|\psi_j^{n+1}|^2 - |\psi_j^n|^2) = 0. \tag{2.23}$$

Then, compute the product of the discrete Schrödinger equation (2.11) with $h(\phi_j^{n+1} - \phi_j^{n-1})$, summing up with j, we obtain

$$\begin{aligned}&\varepsilon^2(\|\phi_t^n\|_2^2 - \|\phi_t^{n-1}\|_2^2) + \frac{1}{2}(\|\phi_x^{n+1}\|_2^2 - \|\phi_x^{n-1}\|_2^2) + \frac{1}{2}(\|\phi^{n+1}\|_2^2 - \|\phi^{n-1}\|_2^2)\\ &- h\sum_{j=1}^{M-1}(\phi_j^{n+1} - \phi_j^{n-1})|\psi_j^n|^2 = 0.\end{aligned} \tag{2.24}$$

Combine (2.23) and (2.24), and noticing

$$\begin{aligned}&h\sum_{j=1}^{M-1}\left((\phi_j^{n+1} + \phi_j^n)(|\psi_j^{n+1}|^2 - |\psi_j^n|^2) + (\phi_j^{n+1} - \phi_j^{n-1})|\psi_j^n|^2\right)\\ &= h\sum_{j=1}^{M-1}\left((\phi_j^{n+1} + \phi_j^n)|\psi_j^{n+1}|^2 - (\phi_j^n + \phi_j^{n-1})|\psi_j^n|^2\right),\end{aligned}$$

which yields

$$\mathcal{E}^n = \mathcal{E}^{n-1}. \tag{2.25}$$

□

From these properties, we can get the following lemma:

Lemma 2.1.2. *Suppose that $\phi(x,t)$ and $\psi(x,t)$ satisfy the assumption A, there exists a constant C, and for h enough small, such that $\|\phi_x^n\|_2 \le C$, $\|\phi^n\|_\infty \le C$, $\|\psi_x^n\|_2 \le C$, $\|\psi^n\|_\infty \le C$.*

Proof. By using the discrete Gagliado-Nirenberg inequality

$$\|u\|_{l^4} \le C\|u\|_{l^2}^{\frac{3}{4}}\|u_x\|_{l^2}^{\frac{1}{4}}, \quad \forall u \in H^1, \tag{2.26}$$

we have

$$\begin{aligned} & h\sum_{j=1}^{M-1}(\phi_j^{n+1})|\psi_j^{n+1}|^2 \\ & \le \|\phi^{n+1}|\psi^{n+1}|\|_2\|\psi^{n+1}\|_2 \\ & \le \|\phi^{n+1}\|_4\|\psi^{n+1}\|_4\|\psi^{n+1}\|_2 \\ & \le C\|\phi^{n+1}\|_2^{3/4}\|\phi_x^{n+1}\|_2^{1/4}\|\psi_x^{n+1}\|_2^{1/4}\|\psi^{n+1}\|_2^{7/4} \\ & \le \frac{1}{2}(\|\phi^{n+1}\|_2^2 + \|\phi_x^{n+1}\|_2^2 + \|\psi_x^{n+1}\|_2^2) + C\|\psi^{n+1}\|_2^{14/3}, \end{aligned} \tag{2.27}$$

with the help of Young's inequality.

According to the assumption on the initial data, there exists a constant $C > 0$, independent of ε, such that $\mathcal{E}^0 \le C$, $\|\psi^0\|_2^2 \le C$. Since $\mathcal{E}^n = \mathcal{E}^0$ and $\|\psi^n\|_2^2 = \|\psi^0\|_2^2$, and together with (2.27), we can have

$$\begin{aligned} & \varepsilon^2\|\phi_t^n\|_2^2 + \frac{1}{2}(\|\phi_x^n\|_2^2 + \|\phi_x^{n+1}\|_2^2) + \frac{1}{2}(\|\phi^n\|_2^2 + \|\phi^{n+1}\|_2^2) \\ & + 2\|\psi_x^{n+1}\|_2^2 \le C_1\mathcal{E}^0 + C_2\|\psi^0\|_2^2 \le C, \end{aligned} \tag{2.28}$$

which implies that $\|\phi_x^n\|_{H^1} \le C$ and $\|\psi_x^n\|_{H^1} \le C$, such that $\|\phi^n\|_\infty \le C$, $\|\psi^n\|_\infty \le C$. □

2.1.2 Convergence analysis when $\varepsilon = 1$

Here we give the convergence results of the ECFD method in the regime: $\varepsilon = O(1)$. Without loss of generality and for the simplicity of notation, we set $\varepsilon = 1$ in this subsection. Define the grid error function as

$$e_j^n = \psi(x_j,t_n) - \psi_j^n, \ \eta_j^n = \phi(x_j,t_n) - \phi_j^n. \tag{2.29}$$

For the above conservative scheme (ECFD), we can establish the following error estimate:

Theorem 2.1.1. *Assume $k \lesssim h$ and under assumptions (A), there exist constants $k_0 > 0$ and $h_0 > 0$ sufficiently small such that,when $0 < k \le k_0$ and $0 < h < h_0$, we have the following error estimate for the ECFD scheme (2.10-2.14) when $\varepsilon = 1$:*

$$\|e^n\|_{H^1} \lesssim h^2 + k^2, \ \|\eta^n\|_{H^1} \lesssim (h^2 + k^2), \ 0 \le n \le \frac{T}{k}.$$

In order to prove Theorem 2.1.1, we first establish the following lemmas. Define θ_j^n and δ_j^n as the truncation errors of the scheme (2.10)-(2.14), which are written as follows

$$\begin{aligned}\theta_j^n &= i(\psi(x_j,t_n))_t + \frac{1}{2}(\psi(x_j,t_{n+1}) + \psi(x_j,t_n))_{x\bar{x}} \\ &+ \frac{1}{4}[\phi(x_j,t_{n+1}) + \phi(x_j,t_n)][\psi(x_j,t_{n+1}) + \psi(x_j,t_n)], \ 1 \le j \le M-1,\end{aligned} \tag{2.30}$$

$$\begin{aligned}\delta_j^n &= \varepsilon^2\phi(x_j,t_n)_{t\bar{t}} - \frac{1}{2}(\phi(x_j,t_{n+1}) + \phi(x_j,t_{n-1}))_{x\bar{x}} \\ &+ \frac{1}{2}(\phi(x_j,t_{n+1}) + \phi(x_j,t_{n-1})) - |\psi(x_j,t_n)|^2, \ 1 \le j \le M-1, \ n \ge 1,\end{aligned} \tag{2.31}$$

$$\delta_j^0 = \phi(x_j,t_0)_t - \phi^{(1)}(x_j) - \frac{k}{2\varepsilon^2}(\partial_{xx}\phi^{(0)}(x_j) - \beta\phi^{(0)}(x_j) + |\psi^{(0)}(x_j)|^2), \tag{2.32}$$

$$\psi(x_j,0) = \psi^{(0)}(x_j), \ \phi(x_j,0) = \phi^{(0)}(x_j), \ 0 \le j \le M, \tag{2.33}$$

$$\psi(a,t_n) = \psi(b,t_n), \ \phi(a,t_n) = \phi(b,t_n), \ n \ge 0. \tag{2.34}$$

Using the Taylor's expansion, we can prove the following lemma:

Lemma 2.1.3. *(Local truncation error of ECFD) $\psi(x,t), \phi(x,t)$ are the solutions of the KGS equations and satisfy the assumption (A), then the truncation errors of the ECFD satisfy*

$$\|\theta^n\|_2 + \|\theta_x^n\|_2 \lesssim h^2 + k^2, \ n = 0, 1, 2\cdots, \tag{2.35}$$

$$\|\delta^n\|_2 + \|\delta_x^n\|_2 \lesssim h^2 + k^2, \quad n = 1, 2\cdots, \tag{2.36}$$

$$\|\delta^0\|_2 + \|\delta_x^0\|_2 \lesssim k^2. \tag{2.37}$$

Similarly, for the SIFD method, we have the same approximation of the truncation error, especially when $\varepsilon = 1$.

From (2.1)-(2.5) and (2.10)-(2.14), and the definition of truncation errors, we obtain the following error equations:

$$i\frac{e_j^{n+1}-e_j^n}{k}+\frac{1}{2}(e_j^{n+1}+e_j^n)_{x\bar{x}}+G_j^n=\theta_j^n,\ 0\le j\le M-1,\ n\ge 0, \tag{2.38}$$

$$\begin{aligned}&\frac{\eta_j^{n+1}-2\eta_j^n+\eta_j^{n-1}}{k^2}-\frac{1}{2}(\eta_j^{n+1}+\eta_j^{n-1})_{x\bar{x}}+\frac{1}{2}(\eta_j^{n+1}+\eta_j^{n-1})\\&-(|\psi(x_j,t_n)|^2-|\psi_j^n|^2)=\delta_j^n,\ 0\le j\le M-1,\ n\ge 1,\end{aligned} \tag{2.39}$$

$$\eta_j^1=k\delta_j^0, e_j^0=0, \eta_j^0=0,\ 0\le j\le M, \tag{2.40}$$

$$e_0^n=e_M^n, \eta_0^n=\eta_M^n,\ e_{-1}^n=e_{M-1}^n, \eta_{-1}^n=\eta_{M-1}^n\ n\ge 0, \tag{2.41}$$

where

$$\begin{aligned}G_j^n&=\frac{1}{4}(\phi(x_j,t_{n+1})+\phi(x_j,t_n))(\psi(x_j,t_{n+1})+\psi(x_j,t_n))\\&-\frac{1}{4}(\phi_j^{n+1})+\phi_j^n)(\psi_j^{n+1}+\psi_j^n)\\&=\frac{1}{4}(\eta_j^n+\eta_j^{n+1})(\psi(x_j,t_{n+1})+\psi(x_j,t_n))+\frac{1}{4}(\phi_j^{n+1}+\phi_j^n)(e_j^{n+1}+e_j^n).\end{aligned}$$

Since the first step calculations are different with the others, we can do the error estimate at the first step.

Lemma 2.1.4. *(Error bounds at $n = 1$). Assume $k \lesssim h$ and under assumptions (A), there exist constants $k_0 > 0$ and $h_0 > 0$ sufficiently small, such that, when $0 < k \le k_0$ and $0 < h < h_0$, we have the following error estimate for the ECFD scheme (2.10) and (2.11) when $n = 1$:*

$$\|e^1\|_{H^1}+\|\eta^1\|_{H^1}\lesssim k^2+h^2. \tag{2.42}$$

Proof. By definition, $e^0 = \mathbf{0} \in \mathbb{R}^{M+1}$. When $n = 1$, from (2.40), we can get the first step error approximation of η^1 from Hölder inequality

$$\|\eta^1\|_2^2\le Ck^2(\|\delta^0\|_2^2). \tag{2.43}$$

and from $(\eta_j^1)_x = k(\delta_j^0)_x$, we can get

$$\|\eta_x^1\|_2^2 \le Ck^2(\|\delta_x^0\|_2^2). \tag{2.44}$$

Next, let $n = 0$ in (2.38) and multiply $h \cdot e_j^1$ on both side of it. Summing up with j, we have

$$\begin{aligned} &\frac{i}{k}\|e^1\|_2^2 - \frac{1}{2}\|e_x^1\|_2^2 + \frac{h}{4}\sum_{j=1}^{M-1}(\phi_j^0 + \phi_j^1)|e_j^1|^2 \\ &+ \frac{h}{4}\sum_{j=1}^{M-1}(\psi(x_j,0) + \psi(x_j,t_1))(\eta_j^1\bar{e}_j^1) = (\theta^0, e^1). \end{aligned} \tag{2.45}$$

Taking the imaginary part of (2.45), we have the following estimation:

$$\begin{aligned} \frac{\|e^1\|_2^2}{k} &= Im(\theta^0, e^1) - Im\left\{\frac{h}{4}\sum_{j=1}^{M-1}(\psi(x_j,0) + \psi(x_j,t_1))(\eta_j^1\bar{e}_j^1)\right\} \\ &\le Ck(\|\theta^0\|_2^2 + \|\eta^1\|_2^0) + \frac{1}{4k}\|e^1\|_2^2. \end{aligned} \tag{2.46}$$

Thus,

$$\|e^1\|_2^2 \le Ck^2(\|\theta^0\|_2^2 + \|\eta^1\|_2^2). \tag{2.47}$$

Taking the real part of (2.45), we obtain

$$\begin{aligned} &\frac{1}{2}\|e_x^1\|_2^2 - \frac{h}{4}\sum_{j=1}^{M-1}(\phi_j^0 + \phi_j^1)|e_j^1|^2 - Re\left\{\frac{h}{4}\sum_{j=1}^{M-1}(\psi^{(0)}(x_j) + \psi(x_j,t_1))(\eta_j^1\bar{e}_j^1)\right\} \\ &= Re(\theta^0, e^1). \end{aligned} \tag{2.48}$$

Similarly, we can get

$$\|e_x^1\|_2^2 \le C(\|\theta^0\|_2^2 + \|\eta^1\|_2^2 + \|e^1\|_2^2). \tag{2.49}$$

Totally, we have the result in the lemma. The proof is complete. □

We start the proof of Theorem 2.1.1. This proof is divided into three steps.

Proof. Step 1. Computing the product of (2.38) with $h(\bar{e}_j^{n+1}+\bar{e}_j^n)$, summing up with j and taking the imaginary part, one obtains

$$\frac{1}{k}(\|e^{n+1}\|_2^2-\|e^n\|_2^2)+Im(G^n,e^n+e^{n+1})=Im(\theta^n,e^n+e^{n+1}),\ n\geq 1. \tag{2.50}$$

From lemma 2.1.2 and Hölder inequality, we have

$$\begin{aligned}|Im(G^n,e^n+e^{n+1})|&\leq C(\|G^n\|_2^2+\|e^n\|_2^2+\|e^{n+1}\|_2^2)\\&\leq(\|e^n\|_2^2+\|e^{n+1}\|_2^2+\|\eta^n\|_2^2+\|\eta^{n+1}\|_2^2),\end{aligned} \tag{2.51}$$

$$|Im(\theta^n,e^n+e^{n+1})|\leq C(\|\theta^n\|_2^2+\|e^n\|_2^2+\|e^{n+1}\|_2^2). \tag{2.52}$$

This implies

$$\|e^{n+1}\|_2^2-\|e^n\|_2^2\leq Ck(\|\eta^{n+1}\|_2^2+\|\eta^n\|_2^2+\|e^{n+1}\|_2^2+\|e^n\|_2^2+\|\theta^n\|_2^2). \tag{2.53}$$

Step 2. Computing the product of (2.38) with $-2h(\bar{e}_j^{n+1}-\bar{e}_j^n)$ and taking the real part, we obtain

$$(\|e_x^{n+1}\|_2^2-\|e_x^n\|_2^2)=P_1^n-2kRe(\theta^n,e_t^n), \tag{2.54}$$

where

$$P_1^n=2kRe(G^n,e_t^n). \tag{2.55}$$

Taking the complex conjugate of (2.38) yields,

$$(\bar{e}^n)_t=-\frac{i}{2}(\bar{e}_j^{n+1}+\bar{e}_j^n)_{x\bar{x}}-i\bar{G}_j^n+i\bar{\theta}_j^n. \tag{2.56}$$

Taking it into (2.54), we get the following estimation:

$$\begin{aligned}&\|e_x^{n+1}\|_2^2-\|e_x^n\|_2^2\\&\lesssim k(\|e^n\|_2^2+\|e^{n+1}\|_2^2+\|e_x^n\|_2^2+\|e_x^{n+1}\|_2^2+\|\eta^n\|_2^2\\&+\|\eta^{n+1}\|_2^2+\|\eta_x^n\|_2^2+\|\eta_x^{n+1}\|_2^2+\|\theta^n\|_2^2+\|\theta_x^n\|_2^2).\end{aligned} \tag{2.57}$$

Step 3. Computing the product of (2.39) with $h(\eta_j^{n+1}-\eta_j^{n-1})$ when $n\geq 1$, summing up with j, we have

$$\begin{aligned}&(\|\eta_t^n\|_2^2-\|\eta_t^{n-1}\|_2^2)+\frac{1}{2}(\|\eta_x^{n+1}\|_2^2-\|\eta_x^{n-1}\|_2^2)+\frac{1}{2}(\|\eta^{n+1}\|_2^2-\|\eta^{n-1}\|_2^2)\\&=(\delta^n,\eta^{n+1}-\eta^{n-1})+h\sum_{j=1}^{M-1}(|\psi(x_j,t_n)|^2-|\psi_j^n|^2)(\eta_j^{n+1}-\eta_j^{n-1}),\ n\geq 1.\end{aligned} \tag{2.58}$$

By Hölder inequality, we obtain

$$\begin{aligned}
&(\|\eta_t^n\|_2^2 - \|\eta_t^{n-1}\|_2^2) + \frac{1}{2}(\|\eta_x^{n+1}\|_2^2 - \|\eta_x^{n-1}\|_2^2) + \frac{1}{2}(\|\eta^{n+1}\|_2^2 - \|\eta^{n-1}\|_2^2) \\
&= (\delta^n, \eta^{n+1} - \eta^{n-1}) + h\sum_{j=1}^{M-1}(|\psi(x_j,t_n)|^2 - |\psi_j^n|^2)(\eta_j^{n+1} - \eta_j^{n-1}) \qquad (2.59) \\
&\le Ck(\|\delta^n\|_2^2 + \|\eta_t^n\|_2^2 + \|\eta_t^{n-1}\|_2^2 + \|e^n\|_2^2).
\end{aligned}$$

Define

$$\mathcal{S}^n = \|e^{n+1}\|_2^2 + \|e_x^{n+1}\|_2^2 + \|\eta_t^n\|_2^2 + \frac{1}{2}(\|\eta^{n+1}\|_2^2 + \|\eta^n\|_2^2) + \frac{1}{2}(\|\eta_x^{n+1}\|_2^2 + \|\eta_x^n\|_2^2). \qquad (2.60)$$

Together with (2.53), (2.57) and (2.59), we obtain

$$\mathcal{S}^n - \mathcal{S}^{n-1} \le Ck(\mathcal{S}^n + \mathcal{S}^{n-1} + (h^2+k^2)^2),\ n \ge 1. \qquad (2.61)$$

Hence, by Gronwall inequality and Lemma 2.1.4, we have

$$\mathcal{S}^n \lesssim (h^2+k^2)^2, \qquad (2.62)$$

which implies

$$\|e^n\|_{H^1} \lesssim h^2+k^2,\quad \|\eta^n\|_{H^1} \lesssim (h^2+k^2),\ 0 \le n \le \frac{T}{k}. \qquad (2.63)$$

□

Remark 2.1.1. *When $0 < \varepsilon \ll 1$, i.e. the singular case, it is very challenging to establish error estimate because of the coupling of two nonlinear terms in the KGS equations and the small parameters ε. However, we can show the error bound numerically.*

Remark 2.1.2. *The convergence analysis results of SIFD scheme are very similar to those of ECFD scheme. We leave out the proof for brevity.*

2.2 Crank-Nicolson time-splitting Fourier pseudospectral method

Now, we are going to study one classical numerical method: the time-splitting method for temporal discretizations, coupled with the Fourier pseudospectral method for spatial discretizations. This method is widely used to solve the nonlinear Schrödinger equation (NLSE) [3] and semiclassical NLSE [12, 22]. The basic idea of time-splitting method is splitting the evolution system in a proper way so that the nonlinear subproblem can be integrated exactly in time. Here we shall briefly review the scheme.

From time $t = t_n$ to $t = t_{n+1}$, the Schrödinger equation (2.1) is solved in two split steps. First, we solve

$$i\partial_t\psi + \partial_{xx}\psi = 0, \tag{2.64}$$

for the time step of length k, followed by solving

$$i\partial_t\psi + \phi\psi = 0 \tag{2.65}$$

for the same time step. Equation (2.64) will be discretized in space by Fourier pseudospectral method and integrated in time exactly. Integrating (2.65) from $t = t_n$ to t_{n+1}, and approximating the integral of $\phi(x,t)$ on $[t_n, t_{n+1}]$ via the trapezoidal rule, one obtains

$$\psi(x,t_{n+1}) \approx e^{\frac{ik}{2}[\phi(x,t_n)+\phi(x,t_{n+1})]}\psi(x,t_n), \quad a \le x \le b. \tag{2.66}$$

Coupled with different methods to compute the Klein-Gordon equation in the KGS equations, we shall solve equations (2.1)-(2.5) with different schemes. One way to discretize the Klein-Gordon equation (2.2) in the KGS equations is by using a pseudospectral method for spatial derivatives, followed by application of a Crank-Nicolson method for linear/nonlinear terms for time derivatives to improve the resolution capacity of the FD methods [14]. Here we shall briefly review the scheme.

To do the pseudospectral discretization in space, we furthermore introduce the following notations. Let $X_M := span\left\{e^{i\mu_l(x-a)},\ \mu_l = \frac{2\pi l}{b-a},\ l = -\frac{M}{2}\cdots\frac{M}{2}-1\right\};\ Y_M := span\left\{v = (v_0, v_1, \cdots, v_M),\ v_0 = v_M\right\}$. For a general periodic function $v(x)$ on $[a,b]$ and a vector $v \in Y_M$, let $P_M : L^2([a,b]) \to X_M$ be the standard L^2-projection operator onto X_M, $I_M : Y_M \to X_M$ be the trigonometric interpolation operator:

$$(P_M v)(x) = \sum_{l=-M/2}^{M/2-1} \widehat{v}_l e^{i\mu_l(x-a)},\ (I_M v)(x) = \sum_{l=-M/2}^{M/2-1} \widetilde{v}_l e^{i\mu_l(x-a)},\ a \le x \le b, \tag{2.67}$$

where

$$\widehat{v}_l = \frac{1}{b-a}\int_a^b v(x)e^{-i\mu_l(x-a)},\quad \widetilde{v}_l = \frac{1}{M}\sum_{j=0}^{M-1} v_j e^{-i\mu_l(x_j-a)}, \tag{2.68}$$

with v_j interpreted as $v(x_j)$ for a function $v(x)$. It is easy to check that P_M and I_M are identical operators on X_M.

The spectral discretization begins with finding $\phi_M(x,t),\ \psi_M(x,t) \in X_M$ i.e.

$$\phi_M(x,t) = \sum_{l=-\frac{M}{2}}^{\frac{M}{2}-1} (\widehat{\phi})_l(t)e^{i\mu_l(x-a)},\ \psi_M(x,t) = \sum_{l=-\frac{M}{2}}^{\frac{M}{2}-1} (\widehat{\psi})_l(t)e^{i\mu_l(x-a)},\ a \le x \le b, \tag{2.69}$$

such that

$$\varepsilon^2\partial_{tt}\phi_M(x,t) - \Delta(\phi_M(x,t)) + \phi_M(x,t) - P_M(|\psi(x,t)|_M^2) = 0. \tag{2.70}$$

Let $(\psi_M)_j^n$ and $(\phi_M)_j^n$ be the approximations of $\psi_M(x_j,t_n)$ and $\phi_M(x_j,t_n)$ $(j = 0,1,...M,\ n = 0,1,...)$, respectively, and $(\widehat{\psi^n})_l$, $(\widehat{\phi^n})_l$ be the approximations of $(\widehat{\psi})_l(t_n)$, $(\widehat{\phi})_l(t_n)$, respectively. Applying Crank-Nicolson method for time derivatives and then discretizing x axis with mesh size $h = (b-a)/M$, which we mentioned in the above section, one ends up with

$$\begin{aligned}&\varepsilon^2\frac{(\phi_M)_j^{n+1} - 2(\phi_M)_j^n + (\phi_M)_j^{n-1}}{k^2} - D_{xx}^f(\frac{1}{2}(\phi_M)^{n+1} + \frac{1}{2}(\phi_M)^{n-1})_{x=x_j}\\ &+ \frac{1}{2}((\phi_M)_j^{n+1} + (\phi_M)_j^{n-1}) - P_M(|\psi_j^n|_M^2) = 0,\ 0 \le j \le M,\ n \ge 1,\end{aligned} \tag{2.71}$$

where

$$D_{xx}^f v|_x = -\sum_{l=-\frac{M}{2}}^{\frac{M}{2}-1} \mu_l^2 \widehat{v}_l e^{i\mu_l(x-a)}, \tag{2.72}$$

and $\widehat{v}_l$ is the Fourier coefficient of a periodic function, and

$$\mu_l = \frac{2\pi l}{b-a}, \quad \widehat{v}_l = \frac{1}{b-a}\int_a^b v(x)e^{-i\mu_l(x-a)}, \ l = -\frac{M}{2}\cdots\frac{M}{2}-1. \tag{2.73}$$

Plugging (2.69) into (2.71), and using orthogonality of the Fourier basis, we obtain

$$\varepsilon^2 \frac{\widehat{(\phi^{n+1})}_l - 2\widehat{(\phi^n)}_l + \widehat{(\phi^{n-1})}_l}{k^2} - \widehat{(|\psi^n|^2)}_l + (\mu_l^2+1)\left(\frac{1}{2}\widehat{(\phi^{n+1})}_l + \frac{1}{2}\widehat{(\phi^{n-1})}_l\right) = 0. \tag{2.74}$$

Solving the equation, we get

$$\widehat{(\phi^{n+1})}_l = \frac{4\varepsilon^2}{2\varepsilon^2 + k^2(\mu_l^2+1)}\widehat{(\phi^n)}_l - \widehat{(\phi^{n-1})}_l + \frac{2k^2}{2\varepsilon^2 + k^2(\mu_l^2+1)}\widehat{(|\psi^n|^2)}_l. \tag{2.75}$$

Combine the splitting steps via the standard strang splitting, then we have the following discrete schemes:

$$(\phi_M)_j^{n+1} = \sum_{l=-\frac{M}{2}}^{\frac{M}{2}-1} \widehat{(\phi^{n+1})}_l e^{i\mu_l(x_j-a)}, \tag{2.76}$$

$$\psi_j^* = \sum_{l=-\frac{M}{2}}^{\frac{M}{2}-1} e^{ik\mu_l^2/2}\widehat{(\psi^n)}_l e^{i\mu_l(x_j-a)}, \tag{2.77}$$

$$\psi_j^{**} = e^{ik(\phi_j^n+\phi_j^{n+1})/2}\psi_j^*, \tag{2.78}$$

$$(\psi_M)_j^{n+1} = \sum_{l=-\frac{M}{2}}^{\frac{M}{2}-1} e^{-ik\mu_l^2/2}\widehat{(\psi^{**})}_l e^{i\mu_l(x_j-a)}, \ 0 \le j \le M-1, \ n \ge 0, \tag{2.79}$$

where $\widehat{(\phi^{n+1})}_l$ is given in (2.75) for $n > 0$. For $n = 0$, the initial conditions are dicretized as

$$\psi_M^0(x) = \psi^{(0)}(x), \ \phi_M^0 = \phi^{(0)}(x), \ \frac{\phi_M^1 - \phi_M^{-1}}{2k}(x) = \phi^{(1)}(x). \tag{2.80}$$

This implies that

$$\begin{aligned}(\widehat{\phi^1})_l = &\frac{2\varepsilon^2}{2\varepsilon^2+k^2(\mu_l^2+1)}(\widehat{\phi^{(0)}})_l + \frac{k(k^2(\mu_l^2+1)+2\varepsilon^2)}{2\varepsilon^2+k^2(\mu_l^2+1)}(\widehat{\phi^{(1)}})_l\\ &+\frac{k^2}{2\varepsilon^2+k^2(\mu_l^2+1)}(\widehat{|\psi^0|^2})_l, \quad l=-\frac{M}{2},\cdots,\frac{M}{2}-1.\end{aligned} \tag{2.81}$$

and

$$(\widehat{\psi^1})_l = (1-ik\mu_l^2)(\widehat{\psi^{(0)}}) + ik(\widehat{\psi^{(0)}\phi^{(0)}}), \tag{2.82}$$

which is conducted from the original Schrödinger equation.

The above procedure is not suitable in practice due to the difficulty of calculating the integrals determining the Fourier transform coefficients $\widehat{v}_l$ defined in (2.68) of a periodic function $v(x)$. Here, we adopt an efficient implementation by choosing $\psi_j^0,\ \phi_j^0$ and $(\phi_t)_j^0$ as the interpolations of $\psi^{(0)}(x_j),\ \phi^{(0)}(x_j)$ and $\phi^{(1)}(x_j)$ on the grids, respectively, i.e.,

$$\psi_j^0 = \sum_{l=-\frac{M}{2}}^{\frac{M}{2}-1}(\widetilde{\psi^{(0)}})_l e^{i\mu_l(x_j-a)}, \quad \phi_j^0 = \sum_{l=-\frac{M}{2}}^{\frac{M}{2}-1}(\widetilde{\phi^{(0)}})_l e^{i\mu_l(x_j-a)},$$

$$(\partial_t\phi)_j^0 = \sum_{l=-\frac{M}{2}}^{\frac{M}{2}-1}(\widetilde{\phi^{(1)}})_l e^{i\mu_l(x_j-a)}.$$

Let ψ_j^n and ϕ_j^n be the approximations of $\psi(x_j,t_n)$ and $\phi(x_j,t_n)$ $(j=0,1,...M,\ n=0,1,...)$. The Crank-Nicolson time-splitting Fourier pseudospectral method (C-NTSFP) reads

$$\phi_j^{n+1} = \sum_{l=-\frac{M}{2}}^{\frac{M}{2}-1}(\widetilde{\phi^{n+1}})_l e^{i\mu_l(x_j-a)}, \tag{2.83}$$

$$\psi_j^{*} = \sum_{l=-\frac{M}{2}}^{\frac{M}{2}-1} e^{ik\mu_l^2/2}(\widetilde{\psi^{n}})_l e^{i\mu_l(x_j-a)}, \tag{2.84}$$

$$\psi_j^{**} = e^{ik(\phi_j^n+\phi_j^{n+1})/2}\psi_j^{*}, \tag{2.85}$$

$$\psi_j^{n+1} = \sum_{l=-\frac{M}{2}}^{\frac{M}{2}-1} e^{-ik\mu_l^2/2}(\widetilde{\psi^{**}})_l e^{i\mu_l(x_j-a)},\ 0\le j\le M-1,\ n\ge 0, \tag{2.86}$$

$$\psi_M^n = \psi_0^n,\ \phi_M^n = \phi_0^n,\ n\ge 0, \tag{2.87}$$

where, for $n = 0$,

$$\begin{aligned}(\widetilde{\phi^1})_l = &\frac{2\varepsilon^2}{2\varepsilon^2 + k^2(\mu_l^2+1)}(\widetilde{\phi^{(0)}})_l + \frac{k(k^2(\mu_l^2+1)+2\varepsilon^2)}{2\varepsilon^2 + k^2(\mu_l^2+1)}(\widetilde{\phi^{(1)}})_l \\ &+ \frac{k^2}{2\varepsilon^2 + k^2(\mu_l^2+1)}(\widetilde{|\psi^0|^2})_l,\ l = -\frac{M}{2}, \cdots, \frac{M}{2}-1,\end{aligned} \tag{2.88}$$

$$(\widetilde{\psi^1})_l = (1 - ik\mu_l^2)(\widetilde{\psi^{(0)}}) + ik(\widetilde{\psi^{(0)}\phi^{(0)}}), \tag{2.89}$$

and for $n \geq 1$,

$$(\widetilde{\phi^{n+1}})_l = \frac{4\varepsilon^2}{2\varepsilon^2 + k^2(\mu_l^2+1)}(\widetilde{\phi^n})_l - (\widetilde{\phi^{n-1}})_l + \frac{2k^2}{2\varepsilon^2 + k^2(\mu_l^2+1)}(\widetilde{|\psi^n|^2})_l. \tag{2.90}$$

Here $\tilde{v}_l,\ l = -M/2 \cdots M/2 - 1$ are the discrete Fourier transform coefficients for a vector $v \in Y_M$ defined as

$$\widetilde{v}_l = \frac{1}{M}\sum_{j=0}^{M-1} v_j e^{-i\mu_l(x_j - a)}, \quad l = -M/2 \cdots M/2 - 1. \tag{2.91}$$

The above method is explicit and easy to extend to two and three dimensions. The memory cost is $O(M)$ and computational cost per time step is $O(MlnM)$ thanks to the fast Fourier transform algorithm. Note that the spatial discretization error of pseudospectral method is of spectral order accuracy in space and the time discretization error is demonstrated to be second-order accurate in k. This will be shown in the numerical results. We also remark that this method shares the same ε-scalability for temporal step with finite difference methods for the Klein-Gordon equation in the singular limit regime.

2.3 Numerical results and comparisons

In this section, we present numerical results between the proposed spectral method CNTSFP and the classical finite difference methods including ECFD and SIFD. We will compare their accuracy for fixed $\varepsilon = O(1)$ and their meshing strategy in the parameter regime when $0 < \varepsilon \ll 1$. Thus, we firstly present numerical results

of the KGS equations with a solitary wave solution in 1D to compare the accuracy and stability of the different methods described above. Secondly, we also present the numerical examples with different initial conditions, such as the ill-prepared and well-prepared initial data, to demonstrate the accuracy of those methods for solving the KGS equations for $\varepsilon \in (0, 1]$, especially when $0 < \varepsilon \ll 1$. Note that the initial conditions for (2.3) are always chosen such that $|\psi^{(0)}(x)|$, $|\phi^{(0)}(x)|$ and $|\phi^{(1)}(x)|$ decay to zero sufficiently fast as $|x| \to \infty$. We always compute on a domain, which is large enough such that the periodic boundary conditions do not introduce a significant aliasing error relative to the problem in the whole space.

2.3.1 Accuracy tests

Example 1. The well-known solitary-wave solutions of the KGS equations in this case are

$$\psi(x,t) = \frac{3}{2\sqrt{1-q^2\varepsilon^2}} sech^2\left(\frac{1}{2\sqrt{1-q^2\varepsilon^2}}(x-qt)\right) e^{(iq/2x+Ct)}, \tag{2.92}$$

$$\phi(x,t) = \frac{3}{2(1-q^2\varepsilon^2)} sech^2\left(\frac{1}{2\sqrt{1-q^2\varepsilon^2}}(x-qt)\right), \ a < x < b, \ t \geq 0, \tag{2.93}$$

where q is a constant and $C = \frac{1}{1-q^2\varepsilon^2} - \frac{q^2}{4}$.
The initial conditions are taken as

$$\psi^{(0)}(x) = \psi(x,0), \ \phi^{(0)}(x) = \phi(x,0), \ \phi^{(1)}(x) = \partial_t\phi(x,0), \ a < x < b, \tag{2.94}$$

where $\psi(x,0)$, $\phi(x,0)$, and $\partial_t\phi(x,0)$ are obtained from (2.92) and (2.93) by setting t=0.

We choose $q = 0.5$ in (2.92)-(2.93) and fix $\varepsilon = \frac{1}{16}$ to do the accuracy tests for all the methods. Here we test the spatial and temporal discretization error and the stability constraint of different numerical methods. We solve the problem on the interval $[-40, 40]$, i.e.,$a = -40$ and $b = 40$ with periodic boundary conditions. Let $\psi_{h,k}$ and $\phi_{h,k}$ be the numerical solutions of the system (2.1-2.5) with the initial conditions (2.94) by using a numerical method with mesh size h and time step k.

Table 2.1: Spacial error analysis for $e_{h,k}$ of different methods at $T = 2$ with $k = 0.0001$ for different h.

$e_{h,k}$	$h_0 = 1$	$h_0/2$	$h_0/4$	$h_0/8$	$h_0/16$
ECFD	8.32E-01	1.73E-1	4.16E-2	1.03E-2	2.57E-3
SIFD	8.32E-01	1.73E-1	4.16E-2	1.03E-2	2.57E-3
CNTSFP	5.54E-03	1.03E-7	1.00E-11	8.64E-12	–

Table 2.2: Temporal error analysis for $e_{h,k}$ of different methods at $T = 2$ for different k.

$e_{h,k}$	$k_0 = 0.2$	$k_0/2$	$k_0/4$	$k_0/8$	$k_0/16$	$k_0/32$
ECFD	3.73E-1	9.72E-2	2.69E-2	6.63E-3	1.65E-3	4.12E-4
SIFD	3.56E-1	7.45E-2	1.89E-2	4.60E-3	1.14E-3	2.87E-4
CNTSFP	2.59E-2	6.84E-3	1.69E-3	4.23E-4	1.06E-4	2.64E-5

To quantify the numerical methods, we define the error function as

$$e_{h,k} = \|\psi(\cdot,t) - \psi_{h,k}(t)\|_{H^1} + \|\phi(\cdot,t) - \phi_{h,k}(t)\|_{H^1}. \tag{2.95}$$

Firstly, we test the discretization error in space. In order to do this, we choose a very small time step, e.g. $k = 10^{-4}$, such that the error from time discretization is negligible compared to the spatial discretization error, and solve the KGS equations with different methods under different mesh size h. Tab. 2.1 lists the numerical error of $e_{h,k}$ at $t = 2.0$ with different mesh size h under $k = 10^{-4}$ for all methods. Secondly, we test the temporal discretization error. We choose a very small mesh size, e.g. $h = 1/512$ for the CNFD and SIFD and $h = 1/32$ for the spectral method such that the error from spatial discrezation is negligible compared to time discretization. Tab. 2.2 shows the temporal analysis of $e_{h,k}$ at $t = 2.0$ under various time steps k for all methods.

From Tabs. 2.1-2.2, we can know that when $\varepsilon = O(1)$ is fixed, the CNFD

and SIFD are of second order accuracy in space and in time, which verifies our error estimate in Theorem 2.1.1. The CNTSFP is of spectral-order accuracy in space, and is of second-order accuracy in time, which indicates that the method convergence rate is optimal.

2.3.2 Convergence and resolution studies for $0 < \varepsilon \ll 1$

We now consider $\varepsilon \in (0, 1]$ in the KGS equations, in particular, $0 < \varepsilon \ll 1$, i.e. the singular limit regime. We study the temporal and spatial error of the above methods under different mesh sizes and time steps as $\varepsilon \to 0$. By doing so, we mainly want to investigate two questions. The first question is how the convergence of the numerical method is affected by ε when ε decays. The second question is that within the convergence regime, how the error bound depends on ε. Here, we have three types of initial examples to test. Suppose the initial data of the KGS equations are

$$\psi(x,0) = \psi^{(0)}(x) = sech(x)e^{-ix}, \tag{2.96}$$

$$\phi(x,0) = \phi^{(0)}(x) = \phi_0(x,0) + \varepsilon^{\alpha} sech(x), \tag{2.97}$$

$$\partial_t\phi(x,0) = \phi^{(1)}(x) = \partial_t\phi_0(x,0) + \varepsilon^{\beta} sech(x), \tag{2.98}$$

where α and β are nonnegative integers; $\phi_0(x,0) = (-\Delta+I)^{-1}|\psi^{(0)}|^2$ and $\partial_t\phi_0(x,0) = -i(-\Delta + I)^{-1}\nabla \cdot (\psi^{(0)}\nabla\bar{\psi}^{(0)} - \bar{\psi}^{(0)}\nabla\psi^{(0)})$, which come from the SY equations (see [10]). From the introduction part of the classification of initial data, we test the following three examples.

Example 1. Well-prepared initial data. The following initial data are one example of the well-prepared initial data defined in (1.12). Choose (2.3) as

$$\psi(x,0) = \psi^{(0)}(x) = sech(x)e^{-ix}, \tag{2.99}$$

$$\phi(x,0) = \phi^{(0)}(x) = \phi_0(x,0) + \varepsilon^2 sech(x), \tag{2.100}$$

$$\partial_t\phi(x,0) = \phi^{(1)}(x) = \partial_t\phi_0(x,0) + \varepsilon sech(x). \tag{2.101}$$

We solve the problem on $[-80, 80]$, i.e. $a = -80, b = 80$. Let ψ_g and ϕ_g be the 'exact' solution of (2.1) and (2.2), which are obtained numerically by using different

methods with a very fine mesh, for example $h = 1/512$ and a very small time step $k = 10^{-4}$ for the CNFD and SIFD, and $h = 1/32$, $k = 10^{-6}$ for the CNTSFP. We use the $\psi_{h,k}$ and $\phi_{h,k}$ to represent the numerical solutions with different methods. Define the error function as

$$e_{h,k} = \|\psi_g(t) - \psi_{h,k}(t)\|_2 + \|\phi_g(t) - \phi_{h,k}(t)\|_2. \tag{2.102}$$

Here we test the spatial and temporal discretization error and the stability constraint of different numerical methods. We test the discretization error in time by choosing a very small mesh size, e.g. $h = 1/512$ for the CNFD and SIFD and $h = 1/32$ for the spectral method such that the error from spatial discrezation is negligible compared to time discretization. Similarly, we test the discretization error in space by choosing a very small time step, e.g. $k = 10^{-4}$, such that the error from time discretization is negligible compared to the spatial discretization error.

As for the spatial error, from our numerical experience and estimates in other literature, the spatial and temporal errors of ECFD and SIFD are very similar due to the finite difference discretization, and ECFD is better than SIFD. Thus here we omit the error test of SIFD for brevity and tabulate the spatial and temporal errors of ECFD and CNTSFP with different ε. Tabs. 2.3-2.4 show the spatial errors of ECFD and CNTSFP, respectively, with different ε and time step h at time $t = 2$. Tabs. 2.5-2.6 show the temporal errors of ECFD and CNTSFP, respectively, with different ε and time step k. To study the temporal accuracy of the numerical methods inside the convergence regime, we plot the temporal discretization errors of ECFD and CNTSFP as functions of k for some fixed ε in log-scale. The result is shown in Fig. 2.1.

As is shown in Tabs. 2.3-2.6 and Fig. 2.1, ECFD, SIFD and CNTSFP are uniformly accurate in time and space for solving the well-prepared initial data problem. The ε-scalability of each method is $k = O(1)$ and $h = O(1)$ when $0 < \varepsilon \ll 1$. Moreover, all the methods have second order convergence rate in time for all ε. ECFD and SIFD are of second order accuracy in space and CNTSFP is of spectral order accuracy in space.

Table 2.3: Spatial error analysis for $e_{h,k}$ of ECFD at $T = 2$ with well-prepared initial data.

ECFD	$h_0 = 0.5$	$h_0/2$	$h_0/4$	$h_0/8$	$h_0/16$	$h_0/32$
$\varepsilon_0 = 1$	2.61E-1	8.16E-2	2.23E-2	5.68E-3	1.42E-3	3.56E-4
$\varepsilon_0/2$	3.84E-1	1.12E-1	3.00E-2	7.61E-3	1.91E-3	4.77E-4
$\varepsilon_0/2^2$	4.33E-1	1.21E-1	3.19E-2	8.07E-3	2.02E-3	5.05E-4
$\varepsilon_0/2^3$	4.12E-1	1.22E-1	3.27E-2	8.27E-3	2.07E-3	5.18E-4
$\varepsilon_0/2^4$	4.11E-1	1.22E-1	3.28E-2	8.30E-3	2.08E-3	5.20E-4
$\varepsilon_0/2^5$	4.11E-1	1.22E-1	3.28E-2	8.31E-3	2.08E-3	5.21E-4
$\varepsilon_0/2^6$	4.10E-1	1.22E-1	3.28E-2	8.32E-3	2.08E-3	5.21E-4
$\varepsilon_0/2^7$	4.10E-1	1.22E-1	3.27E-2	8.31E-3	2.08E-3	5.21E-4

Table 2.4: Spatial error analysis for $e_{h,k}$ of CNTSFP at $T = 2$ with well-prepared initial data.

CNTSFP	$h_0 = 1$	$h_0/2$	$h_0/4$	$h_0/8$
$\varepsilon_0 = 1$	7.06E-2	3.74E-4	2.12E-8	6.56E-12
$\varepsilon_0/2$	7.61E-2	4.00E-4	2.25E-8	7.40E-12
$\varepsilon_0/2^2$	7.03E-2	4.18E-4	2.33E-8	7.52E-12
$\varepsilon_0/2^3$	6.17E-2	4.64E-4	2.37E-8	6.75E-12
$\varepsilon_0/2^4$	6.04E-2	4.39E-4	2.39E-8	8.73E-12
$\varepsilon_0/2^5$	6.00E-2	4.37E-4	2.42E-8	9.16E-12
$\varepsilon_0/2^6$	5.99E-2	4.34E-4	2.41E-8	9.03E-12
$\varepsilon_0/2^7$	5.99E-2	4.34E-4	2.41E-8	7.74E-12
$\varepsilon_0/2^8$	5.99E-2	4.32E-4	2.39E-8	6.86E-12
$\varepsilon_0/2^9$	5.99E-2	4.32E-4	2.39E-8	6.68E-12

Table 2.5: Temporal error analysis for $e_{h,k}$ of ECFD at $T = 2$ with well-prepared initial data.

ECFD	$k_0 = 0.2$	$k_0/2^2$	$k_0/2^4$	$k_0/2^5$	$k_0/2^6$	$k_0/2^7$
$\varepsilon_0 = 1$	3.48E-1	3.89E-2	2.50E-3	6.25E-4	1.56E-4	3.90E-5
$\varepsilon_0/2$	6.11E-1	5.69E-2	4.11E-3	1.04E-3	2.62E-4	6.98E-5
$\varepsilon_0/2^2$	7.23E-1	7.19E-2	5.15E-3	1.29E-3	3.26E-4	8.57E-5
$\varepsilon_0/2^3$	6.56E-1	6.71E-2	5.53E-3	1.40E-3	3.54E-4	9.25E-5
$\varepsilon_0/2^4$	6.35E-1	5.41E-2	5.55E-3	1.51E-3	3.89E-4	1.02E-4
$\varepsilon_0/2^5$	6.34E-1	5.19E-2	5.12E-3	1.55E-3	8.11E-4	6.78E-4
$\varepsilon_0/2^6$	6.48E-1	5.60E-2	4.85E-3	1.20E-3	5.24E-4	3.69E-4
$\varepsilon_0/2^7$	6.52E-1	5.28E-2	3.93E-3	9.83E-4	3.05E-4	1.42E-4
$\varepsilon_0/2^8$	6.53E-1	5.35E-2	3.95E-3	9.82E-4	2.53E-4	8.28E-5
$\varepsilon_0/2^9$	6.54E-1	5.52E-2	4.10E-3	1.01E-3	2.47E-4	6.62E-5

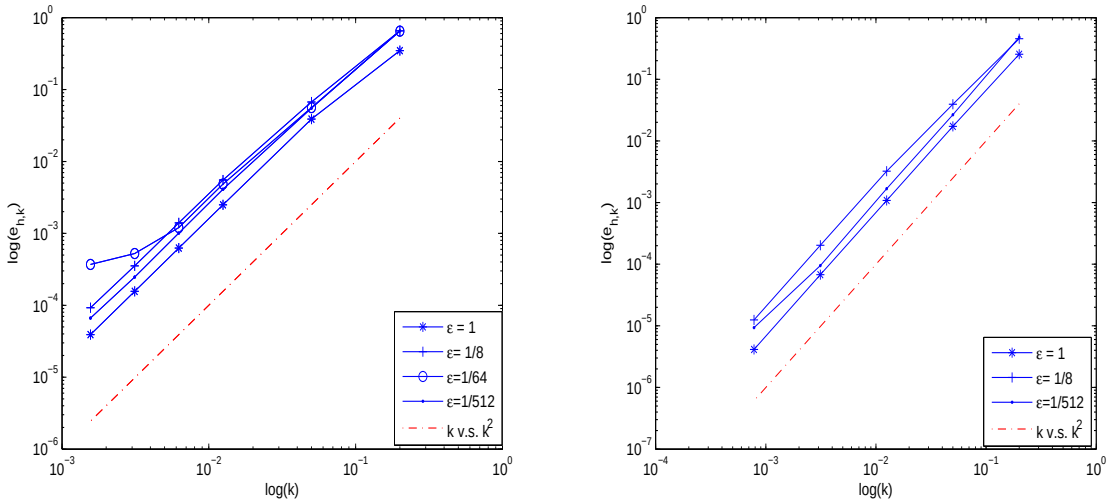

Figure 2.1: Dependence of the temporal discretization errors of ECFD (left) and CNTSFP (right) on k at $t = 2$ with different ε.

Table 2.6: Temporal error analysis for $e_{h,k}$ of CNTSFP at $T = 2$ with well-prepared initial data.

CNTSFP	$k_0 = 0.2$	$k_0/2^2$	$k_0/2^4$	$k_0/2^6$	$k_0/2^8$
$\varepsilon_0 = 1$	2.54E-1	1.72E-2	1.08E-3	6.77E-5	4.13E-6
$\varepsilon_0/2$	4.73E-1	3.15E-2	1.96E-3	1.22E-4	7.52E-6
$\varepsilon_0/2^2$	5.30E-1	4.58E-2	2.87E-3	1.78E-4	1.09E-5
$\varepsilon_0/2^3$	4.55E-1	3.93E-2	3.22E-3	2.03E-4	1.25E-5
$\varepsilon_0/2^4$	4.52E-1	2.60E-2	3.17E-3	2.35E-4	1.44E-5
$\varepsilon_0/2^5$	4.59E-1	2.36E-2	2.70E-3	3.70E-4	2.48E-5
$\varepsilon_0/2^6$	4.75E-1	2.72E-2	1.62E-3	4.32E-4	4.25E-5
$\varepsilon_0/2^7$	4.80E-1	2.39E-2	1.55E-3	1.54E-4	5.30E-5
$\varepsilon_0/2^8$	4.81E-1	2.48E-2	1.57E-3	9.75E-5	2.95E-5
$\varepsilon_0/2^9$	4.81E-1	2.65E-2	1.68E-3	9.49E-5	9.35E-6

Example 2. Ill-prepared initial data. The following initial data are one example of the ill-prepared initial data defined in (1.13). Choose (2.3) as

$$\psi(x,0) = \psi^{(0)}(x) = sech(x)e^{-ix}, \tag{2.103}$$

$$\phi(x,0) = \phi^{(0)}(x) = \phi_0(x,0) + \varepsilon sech(x), \tag{2.104}$$

$$\partial_t\phi(x,0) = \phi^{(1)}(x) = \partial_t\phi_0(x,0) + sech(x). \tag{2.105}$$

We solve the problem on $[-280, 280]$, i.e. $a = -280, b = 280$ such that the periodic boundary conditions do not introduce a significant aliasing error relative to the problem in the whole space. The spatial error and temporal error here are computed in a similar way as before. With the ill-prepared initial data, the spatial errors of SIFD, ECFD and CNTSFP are still uniformly accurate, which are very similar to the results shown in Example 1, Tabs. 2.3-2.4. Here, we omit them for brevity. Tabs. 2.7-2.8 show the temporal errors of ECFD and CNTSFP, respectively, under different ε and time step k. To study the error bounds of the numerical methods,

Table 2.7: Temporal error analysis for $e_{h,k}$ of ECFD at time $T = 2$ with ill-prepared initial data.

ECFD	$k_0 = 0.2$	$k_0/2^2$	$k_0/2^4$	$k_0/2^5$	$k_0/2^6$	$k_0/2^7$
$\varepsilon_0 = 1$	3.48E-1	3.89E-2	2.50E-3	6.25E-4	1.56E-4	3.90E-5
$\varepsilon_0/2$	6.07E-1	5.58E-2	4.00E-3	9.92E-4	2.37E-4	5.37E-5
$\varepsilon_0/2^2$	7.66E-1	8.74E-2	6.20E-3	1.54E-3	3.71E-4	8.18E-5
$\varepsilon_0/2^3$	6.71E-1	1.57E-1	1.27E-2	3.20E-3	7.91E-4	1.89E-4
$\varepsilon_0/2^4$	7.53E-1	2.04E-1	3.74E-2	1.06E-2	2.71E-3	6.73E-4
$\varepsilon_0/2^5$	7.11E-1	9.80E-2	7.18E-2	3.28E-2	1.02E-2	2.70E-3
$\varepsilon_0/2^6$	6.30E-1	1.21E-1	3.87E-2	2.81E-2	2.84E-2	9.63E-3
$\varepsilon_0/2^7$	6.98E-1	2.51E-1	1.81E-2	1.63E-2	1.69E-2	3.81E-2

Table 2.8: Temporal error analysis for $e_{h,k}$ of CNTSFP at time $T = 2$ with ill-prepared initial data.

CNTSFP	$k_0 = 0.2$	$k_0/2^2$	$k_0/2^4$	$k_0/2^6$	$k_0/2^8$	$k_0/2^9$
$\varepsilon_0 = 1$	2.54E-1	1.72E-2	1.08E-3	6.77E-5	4.13E-6	9.53E-7
$\varepsilon_0/2$	5.05E-1	3.49E-2	2.19E-3	1.37E-4	8.41E-6	2.00E-6
$\varepsilon_0/2^2$	6.13E-1	6.58E-2	4.29E-3	2.68E-4	1.65E-5	3.92E-6
$\varepsilon_0/2^3$	4.51E-1	1.29E-1	1.04E-2	6.64E-4	4.09E-5	9.73E-6
$\varepsilon_0/2^4$	5.66E-1	1.76E-1	3.50E-2	2.57E-3	1.59E-4	3.79E-5
$\varepsilon_0/2^5$	5.43E-1	6.89E-2	6.94E-2	1.00E-2	6.65E-4	1.58E-4
$\varepsilon_0/2^6$	5.33E-1	9.21E-2	3.63E-2	2.83E-2	2.65E-3	6.45E-4
$\varepsilon_0/2^7$	7.77E-1	2.23E-1	1.57E-2	1.68E-2	8.26E-3	2.42E-3
$\varepsilon_0/2^8$	1.37E+0	1.98E-1	1.81E-2	7.58E-3	6.67E-3	7.15E-3

we plot the dependence of temporal discretization errors of ECFD and CNTSFP on ε for some fixed k in log-scale. The result is shown in Fig. 2.2.

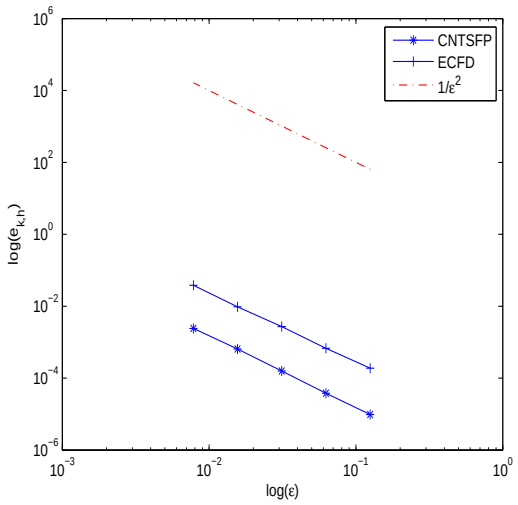

Figure 2.2: Dependence of the temporal discretization errors of ECFD and CNTSFP on ε at $t = 2$ under $k = 1/6400$.

From Tabs. 2.7-2.8 and Fig. 2.2, we can draw the following observations:

1. ECFD, SIFD and CNTSFP have uniformly accuracy in space for all ε (cf. similar to the corresponding columns in Tabs. 2.3, 2.4). The spatial discretization errors are totally independent of ε and the spatial resolution is $h = O(1)$, $0 < \varepsilon \ll 1$.

2. ECFD and SIFD are of second order accuracy in space; CNTSFP is of spectral accuracy in space, and the computation cost is much smaller than ECFD and SIFD since it is explicit.

3. When k is sufficiently small, i.e., within the convergence regime $k \lesssim \varepsilon$, ECFD, SIFD and CNTSFP are second order accurate in time (cf. the upper diagonal parts in Tabs. 2.7, 2.8). All of them have some convergence order reductions or lose the convergence outside the convergence regime (cf. the lower diagonal parts in Tabs. 2.7, 2.8).

4. The temporal discretization error bounds of ECFD, SIFD and CNTSFP within the convergence regime are like $O(\varepsilon^{-2}k^2)$ (cf. Fig. 2.2) and the ε-scalability is $k = O(\varepsilon)$.

Example 3. Extremely ill-prepared initial data. The following initial data are

one example of the extremely ill-prepared initial data defined in (1.14). Choose (2.3) as

$$\psi(x,0) = \psi^{(0)}(x) = sech(x)e^{-ix}, \tag{2.106}$$

$$\phi(x,0) = \phi^{(0)}(x) = \phi_0(x,0) + sech(x), \tag{2.107}$$

$$\partial_t\phi(x,0) = \phi^{(1)}(x) = \partial_t\phi_0(x,0) + sech(x). \tag{2.108}$$

We solve the problem on $[-600, 600]$, i.e. $a = -600, b = 600$ such that the periodic boundary conditions do not introduce a significant aliasing error relative to the problem in the whole space. Again, the spatial error and temporal error here are computed in a similar way as before. Tabs. 2.9-2.10 show the temporal errors of ECFD and CNTSFP, respectively, under different ε and time step k. Again, to study the error bounds of the numerical methods inside the convergence regime, we plot the dependence of temporal discretization errors of ECFD and CNTSFP on ε for some fixed k in log-scale. The result is shown in Fig. 2.3. Tab. 2.11-2.12 show the spatial errors of ECFD and CNTSFP for this example. Since the spacial error of ECFD has a small increase when ε decays, we plot the dependence of the spacial error of ECFD on ε under different h in Fig. 2.4.

Again, from Tabs. 2.9-2.12 and Figs. 2.3-2.4, we can draw the following conclusions:

1. CNTSFP still has uniformly spectral accuracy in space for all ε (cf. each column in Tab. 2.12). The spatial discretization errors are totally independent of ε and the spatial resolution is $h = O(1)$, $0 < \varepsilon \ll 1$.

2. ECFD and SIFD have second-order accuracy spacial error for all ε and the dependence of spatial error on ε is like $1/\sqrt{\varepsilon}$. Thus the spatial resolution is $h = O(\varepsilon^{1/4})$, for $0 < \varepsilon \ll 1$ (cf. Tab. 2.11 and Fig. 2.4).

3. When k is sufficiently small, i.e., within the convergence regime $k \lesssim \varepsilon^{1.5}$, ECFD, SIFD and CNTSFP are second order accurate in time (cf. the upper diagonal parts in Tabs. 2.9, 2.10). All of them have some convergence order reductions or lose the convergence outside the convergence regime (cf. the lower diagonal parts

Table 2.9: Temporal error analysis for $e_{h,k}$ of CNTSFP at $T = 2$ with extremely ill-prepared initial data.

CNTSFP	$k_0 = 0.2$	$k_0/2^2$	$k_0/2^4$	$k_0/2^6$	$k_0/2^8$	$k_0/2^{10}$
$\varepsilon_0 = 1$	2.54E-1	1.72E-2	1.08E-3	6.77E-5	4.13E-6	1.65E-7
$\varepsilon_0/2$	5.50E-1	4.07E-2	2.59E-3	1.62E-4	9.97E-6	4.74E-7
$\varepsilon_0/2^2$	1.27E+0	1.50E-1	1.02E-2	6.43E-4	3.96E-5	1.86E-6
$\varepsilon_0/2^3$	2.40E+0	7.52E-1	7.12E-2	4.58E-3	2.82E-4	1.32E-5
$\varepsilon_0/2^4$	8.53E+0	1.73E+0	4.77E-1	3.68E-2	2.28E-3	1.07E-4
$\varepsilon_0/2^5$	1.56E+1	1.75E+0	1.69E+0	2.72E-1	1.84E-2	8.64E-4
$\varepsilon_0/2^6$	1.64E+1	6.61E+0	1.62E+0	1.33E+0	1.38E-1	6.74E-3
$\varepsilon_0/2^7$	1.70E+1	3.47E+1	2.05E+0	1.65E+0	8.36E-1	5.43E-2
$\varepsilon_0/2^8$	1.68E+1	5.69E+1	7.06E+0	1.36E+0	1.46E+0	3.74E-1

Table 2.10: Temporal error analysis for $e_{h,k}$ of ECFD at $T = 2$ with extremely ill-prepared initial data.

ECFD	$k_0/2^2$	$k_0/2^3$	$k_0/2^4$	$k_0/2^5$	$k_0/2^6$	$k_0/2^7$
$\varepsilon_0 = 1$	3.89E-2	9.93E-3	2.50E-3	6.25E-4	1.56E-4	3.90E-5
$\varepsilon_0/2$	1.90E-1	4.89E-2	1.24E-2	3.10E-3	7.76E-4	1.93E-4
$\varepsilon_0/2^2$	1.05E+0	2.83E-1	7.27E-2	1.83E-2	4.60E-3	1.15E-3
$\varepsilon_0/2^3$	3.72E+0	1.38E+0	3.89E-1	1.00E-1	2.53E-2	6.34E-3
$\varepsilon_0/2^4$	4.48E+0	4.58E+0	2.46E+0	7.63E-1	1.98E-1	5.00E-2
$\varepsilon_0/2^5$	8.36E+0	3.09E+0	3.02E+0	3.92E+0	1.55E+0	4.10E-1
$\varepsilon_0/2^6$	1.70E+1	3.45E+1	2.06E+0	1.44E+0	1.65E+0	1.78E+0
$\varepsilon_0/2^7$	1.69E+1	5.67E+1	7.06E+0	2.10E+0	1.36E+0	1.56E+0

in Tabs. 2.9, 2.10). And when ε is very small, ECFD, SIFD and CNTSFP are not efficient for solving the KGS equations numerically.

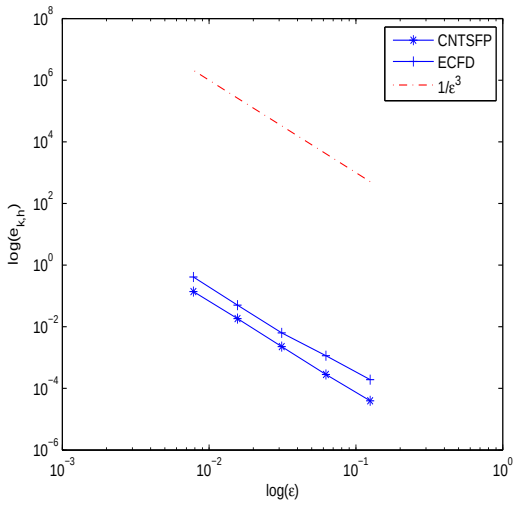

Figure 2.3: Dependence of the temporal discretization errors of ECFD and CNTSFP on ε at $t = 2$ under $k = 1/6400$.

Table 2.11: Spatial error analysis for $e_{h,k}$ of ECFD at $T = 2$ with extremely ill-prepared initial data.

ECFD	$h_0 = 1/4$	$h_0/2$	$h_0/4$	$h_0/8$	$h_0/16$
$\varepsilon_0 = 1$	8.16E-2	2.23E-2	5.68E-3	1.42E-3	3.56E-4
$\varepsilon_0/2$	1.10E-1	2.89E-2	7.30E-3	1.83E-3	4.57E-4
$\varepsilon_0/2^2$	1.46E-1	3.73E-2	9.37E-3	2.34E-3	5.86E-4
$\varepsilon_0/2^3$	1.54E-1	4.23E-2	1.07E-2	2.69E-3	6.73E-4
$\varepsilon_0/2^4$	1.87E-1	5.12E-2	1.30E-2	3.26E-3	8.14E-4
$\varepsilon_0/2^5$	2.47E-1	7.18E-2	1.85E-2	4.63E-3	1.16E-3
$\varepsilon_0/2^6$	3.34E-1	1.09E-1	2.95E-2	7.43E-3	1.86E-3
$\varepsilon_0/2^7$	4.45E-1	1.70E-1	5.04E-2	1.30E-2	3.26E-3

4. The temporal discretization error bounds of ECFD, SIFD and CNTSFP within the convergence regime behave like $O(\varepsilon^{-3}k^2)$ (cf. Fig.2.2) and the ε-scalability is $k = O(\varepsilon^{1.5})$.

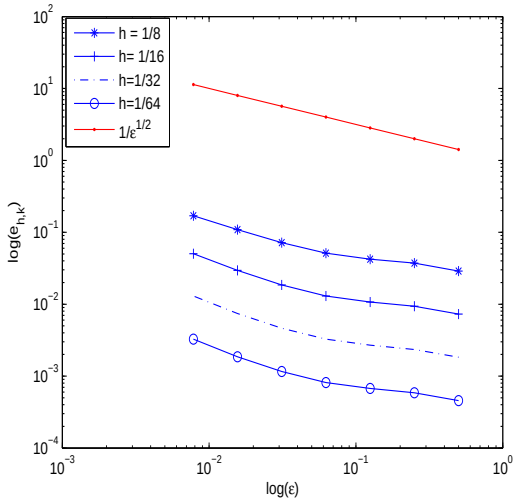

Figure 2.4: Dependence of the spacial discretization error of ECFD on ε at $t = 2$ with different h.

Table 2.12: Spatial error analysis for $e_{h,k}$ of CNTSFP at $T = 2$ with extremely ill-prepared initial data.

CNTSFP	$h_0 = 1$	$h_0/2$	$h_0/4$	$h_0/8$
$\varepsilon_0 = 1$	7.06E-2	3.74E-4	2.12E-8	7.14E-12
$\varepsilon_0/2$	8.82E-2	3.61E-4	2.10E-8	1.05E-11
$\varepsilon_0/2^2$	1.02E-1	3.93E-4	2.19E-8	6.46E-12
$\varepsilon_0/2^3$	7.45E-2	6.35E-4	2.38E-8	8.07E-12
$\varepsilon_0/2^4$	7.77E-2	5.49E-4	3.07E-8	3.97E-11
$\varepsilon_0/2^5$	7.02E-2	5.76E-4	3.14E-8	1.99E-11
$\varepsilon_0/2^6$	7.56E-2	5.00E-4	2.61E-8	9.81E-12
$\varepsilon_0/2^7$	7.53E-2	5.37E-4	3.03E-8	7.57E-12
$\varepsilon_0/2^8$	7.52E-2	5.15E-4	2.98E-8	9.12E-12

From the numerical tests with three examples, we mainly draw the following conclusions:

- All the methods are uniformly accurate in space with different types of initial data except for the ECFD and SIFD methods, which show $h^2/\sqrt{\varepsilon}$ error bound in space for solving extremely ill-prepared data problem. SIFD and ECFD are all of second-order accuracy and CNTSFP is of spectral accuracy.

- All the methods shown in this chapter are efficient for solving the KGS equations in time with well-prepared type initial data for all $\varepsilon \in (0, 1]$, especially when $0 < \varepsilon \ll 1$, which indicates that the solutions to the KGS equations have no oscillation with respect to ε.

- ECFD, SIFD and CNTSFP are efficient and of second-order accuracy in time for solving the KGS equations in the classical regime, i.e., $\varepsilon = O(1)$, with different types of initial data, which are shown in the upper few rows in each table. However, these methods have some convergence order reductions or lose the convergence outside the convergence regime for solving the ill-prepared or extremely ill-prepared problem which are shown from the very lower trigonal parts of temporal analysis tables. These indicate that when ε is very small, these methods are not efficient nor optimal for solving the KGS equations numerically except for taking k sufficiently small.

- The temporal discretization error bounds of ECFD, SIFD and CNTSFP are like $O(\varepsilon^{-2}k^2)$ and $O(\varepsilon^{-3}k^2)$ approximately for solving the KGS equations with ill-prepared and extremely ill-prepared initial data, respectively. The solutions with these two types of initial data are highly oscillatory with respect to ε. The temporal ε-scalability is $k = O(\varepsilon)$ when the initial data are ill-prepared and $k = O(\varepsilon^{1.5})$ when the initial data are extremely ill-prepared, indicating that the existing numerical methods are not efficient for solving the KGS equations in the singular limit regime with ill-prepared or extremely ill-prepared initial data.

Chapter 3

Uniformly accurate numerical methods

In this chapter, we will propose two uniformly accurate, efficient and explicit methods for the KGS equations in the singular limit regime based on the exponential wave integrator method for solving second order nonlinear ODEs. According to the recent work in [8], a Gautschi-type exponential wave integrator (EWI) [42, 46] was used to solve the Klein-Gordon equation in the nonrelativistic limit regime. Gautschi-type exponential integrator methods are widely used for solving wave equations [37] and high oscillation problems [38]. In section 3.1, we are going to propose EWI method to solve the KG equation, coupled with time-splitting Fourier pseudospectral (TSFP) method for solving the Schrödinger equation to solve the KGS equations in the singular limit regime efficiently. Another very similar method is given in section 3.2, which is also an exponential wave integrator Fourier pseudospectral method. Numerical results on two examples are shown in Section 3.3, which shows that the two methods are uniformly accurate for all $\varepsilon \in (0, 1]$.

3.1 Exponential wave integrator (EWI) pseudospectral method

As for the problem (2.1-2.5) in Chapter 2, we already showed some methods which are not uniformly accurate for solving the problem with ill-prepared or extremely ill-prepared initial data, even more, the methods are not efficient when ε is very small. We already stated that we can find some efficient methods for solving the Klein-Gordon equation, and then coupled it with time-splitting method for the Schrödinger equation to solve the KGS equations. Now, we are going to study one method to discretize the Klein-Gordon equation (2.2), which is designed by using the pseudospectral method for spatial derivatives and the Gautschi-type exponential wave integrator method (EWI) for solving the second-order ODEs.

The spectral discretization also begins with finding $\phi_M(x,t),\ \psi_M(x,t) \in X_M$ i.e.

$$\phi_M(x,t) = \sum_{l=-M/2}^{M/2-1} \widehat{\phi}_l(t) e^{i\mu_l(x-a)},\ \psi_M(x,t) = \sum_{l=-M/2}^{M/2-1} \widehat{\psi}_l(t) e^{i\mu_l(x-a)}, \tag{3.1}$$

such that

$$\varepsilon^2 \partial_{tt}\phi_M(x,t) - \Delta(\phi_M(x,t)) + \phi_M(x,t) - P_M(|\psi(x,t)|_M^2) = 0. \tag{3.2}$$

Plugging (3.1) into (3.2), noticing the orthogonality of the Fourier functions, we get the the ODEs:

$$\varepsilon^2 \frac{d^2}{dt^2}\widehat{\phi_l(t)} + (\mu_l^2+1)\widehat{\phi_l(t)} - |\widehat{\psi}|_l^2(t) = 0,\ l = -\frac{M}{2}, \cdots, \frac{M}{2}-1. \tag{3.3}$$

Then a numerical method can be designed by properly treating the above second order ODEs. For each l, around time $t_n = nk$ $(n \geq 0)$, we reformulate the above ODEs as

$$\varepsilon^2 \frac{d^2}{dt^2}\widehat{\phi}_l(t_n+s) + (\mu_l^2+1)\widehat{\phi}_l(t_n+s) - |\widehat{\psi}|_l^2(t_n+s) = 0. \tag{3.4}$$

Denote

$$\beta_l = \frac{\sqrt{\mu_l^2+1}}{\varepsilon}, \quad \widehat{f_l^n}(s) = \widehat{|\psi(t_n+s)|^2}. \tag{3.5}$$

Using variation-of-constant, then the general solution of the above second-order ODEs (3.4) can be written as

$$\widehat{\phi_l}(t_n+s) = c_l^n \cos(\beta_l s) + d_l^n \frac{\sin(\beta_l s)}{\beta_l} + \frac{1}{\varepsilon^2 \beta_l}\int_0^s \widehat{f_l^n(\omega)} \sin(\beta_l(s-\omega))d\omega, \quad (3.6)$$

where c_l^n, d_l^n are two constants to be determined.

When $n=0$ and $s=0$, we plug the initial (2.3) into (3.6), and get the two constants

$$c_l^0 = \widehat{\phi_l^{(0)}} \quad d_l^0 = \frac{d}{dt}\widehat{\phi_l^0}. \quad (3.7)$$

Thus, when $n=0$, we get

$$\widehat{\phi_l}(s) = (\widehat{\phi^{(0)}})_l \cos(\beta_l s) + (\widehat{\phi^{(1)}})_l \frac{\sin(\beta_l s)}{\beta_l} + \frac{1}{\varepsilon^2 \beta_l}\int_0^s \widehat{f_l^n(\omega)} \sin(\beta_l(s-\omega))d\omega. \quad (3.8)$$

When $n>0$, consider the solution in (3.6) for $s\in[-k,k]$ and require the solution to be continuous at $t=t_n$ and $t=t_{n-1}$. Plugging $s=0$ and $s=-k$ into (3.6) to determine the constants c_l^n, d_l^n, and then letting $s=k$, we have

$$\begin{aligned}\widehat{\phi_l}(t_{n+1}) &= 2\widehat{\phi_l}(t_n)\cos(\beta_l k) - \widehat{\phi_l}(t_{n-1}) \\ &\quad + \frac{1}{\varepsilon^2\beta_l}\int_0^k (\widehat{f_l^n(\omega)} + \widehat{f_l^n(-\omega)})\sin(\beta_l(k-\omega))d\omega.\end{aligned} \quad (3.9)$$

We adopt the following Gautschi's type quadrature to approximate the integrals in (3.8) and (3.9)

$$\int_0^k (\widehat{f_l^n(\omega)} + \widehat{f_l^n(-\omega)})\sin(\beta_l(k-\omega))d\omega \approx \frac{2\widehat{f_l^n(0)}}{\beta_l}(1-\cos(\beta_l k)), \quad (3.10)$$

$$\int_0^s \widehat{f_l^0(\omega)}\sin(\beta_l(s-\omega)d\omega \approx \frac{\widehat{f_l^0(0)}(1-\cos(\beta_l k))}{\beta_l} + \frac{k(\beta_l - \sin(\beta_l k))}{\beta_l^2}(\widehat{f_l^0(0)})', \quad (3.11)$$

where $(f^0(0))' = (|\psi^{(0)}|^2)' = i(\partial_{xx}\psi^{(0)}\bar{\psi}^{(0)} - \partial_{xx}\bar{\psi}^{(0)}\psi^{(0)})$ deducted from the exact Schrödinger equation.

Let $\psi_M^n(x_j)$, $\phi_M^n(x_j)$, $(\phi_t)_M^n(x_j)$ as the approximations of $\psi_M(x_j,t_n)$, $\phi_M(x_j,t_n)$ and $\partial_t\phi_M(x_j,t_n)$, respectively; and $\widehat{\psi_l^n}$, $\widehat{\phi_l^n}$ as the approximation of $\widehat{\psi_l}(t_n)$, $\widehat{\phi_l}(t_n)$,

respectively. Combine the split steps via the standard strang splitting, then we have the following discrete scheme:

$$(\phi_M)^{n+1}(x_j) = \sum_{l=-\frac{M}{2}}^{\frac{M}{2}-1} \widehat{\phi_l^{n+1}} e^{i\mu_l(x_j-a)}, \tag{3.12}$$

$$\psi^*(x_j) = \sum_{l=-\frac{M}{2}}^{\frac{M}{2}-1} e^{ik\mu_l^2/2} \widehat{\psi}_l^n e^{i\mu_l(x_j-a)}, \tag{3.13}$$

$$\psi^{**}(x_j) = e^{ik(\phi_j^n+\phi_j^{n+1})/2}\psi_j^*, \tag{3.14}$$

$$(\psi_M)^{n+1}(x_j) = \sum_{l=-\frac{M}{2}}^{\frac{M}{2}-1} e^{-ik\mu_l^2/2} \widehat{\psi_l^{**}} e^{i\mu_l(x_j-a)}, 0 \le j \le M-1, n \ge 0, \tag{3.15}$$

where

$$\begin{aligned} \widehat{\phi_l^1} &= (\widehat{\phi^{(0)}})_l \cos(\beta_l k) + \frac{(\widehat{\phi^{(1)}})_l}{\beta_l} \sin(\beta_l k) + \frac{(1-\cos(\beta_l k))}{\varepsilon^2 \beta_l^2} |\widehat{\psi^{(0)}}|_l^2 \\ &+ (\frac{\beta_l k - k\sin(\beta_l k)}{\beta_l^2})(\widehat{|\psi^0|_l^2})', \end{aligned} \tag{3.16}$$

$$\widehat{\phi_l^{n+1}} = 2\widehat{\phi_l^n}\cos(\beta_l k) - \widehat{\phi_l^{n-1}} + \frac{2(1-\cos(\beta_l k))}{\varepsilon^2\beta_l^2} |\widehat{\psi^n}|_l^2, \; n \ge 1. \tag{3.17}$$

Here, we have the same problem with that in CNTSFP method, that is, it is difficult to compute the integrals defining the Fourier transform coefficients. Thus, we adopt an efficient implementation by choosing ψ_j^0, ϕ_j^0 and $(\phi_t)_j^0$ as the interpolations of $\psi^{(0)}(x_j)$, $\phi^{(0)}(x_j)$ and $\phi^{(1)}(x_j)$ on the grids, respectively, i.e.,

$$\psi_j^0 = \sum_{l=-\frac{M}{2}}^{\frac{M}{2}-1} (\widetilde{\psi^{(0)}})_l e^{i\mu_l(x_j-a)}, \quad \phi_j^0 = \sum_{l=-\frac{M}{2}}^{\frac{M}{2}-1} (\widetilde{\phi^{(0)}})_l e^{i\mu_l(x_j-a)},$$

$$(\partial_t\phi)_j^0 = \sum_{l=-\frac{M}{2}}^{\frac{M}{2}-1} (\widetilde{\phi^{(1)}})_l e^{i\mu_l(x_j-a)}.$$

Let ψ_j^n and ϕ_j^n be the approximations of $\psi(x_j,t_n)$ and $\phi(x_j,t_n)$ ($j=0,1,...M,\ n=0,1,...$). Then the EWI time-splitting Fourier pseudospectral method (EWI-TSFP)

reads

$$\phi_j^{n+1} = \sum_{l=-\frac{M}{2}}^{\frac{M}{2}-1} (\widetilde{\phi^{n+1}})_l e^{i\mu_l(x_j-a)}, \tag{3.18}$$

$$\psi_j^{*} = \sum_{l=-\frac{M}{2}}^{\frac{M}{2}-1} e^{ik\mu_l^2/2} (\widetilde{\psi^{n}})_l e^{i\mu_l(x_j-a)}, \tag{3.19}$$

$$\psi_j^{**} = e^{ik(\phi_j^n+\phi_j^{n+1})/2}\psi_j^{*}, \tag{3.20}$$

$$\psi_j^{n+1} = \sum_{l=-\frac{M}{2}}^{\frac{M}{2}-1} e^{-ik\mu_l^2/2} (\widetilde{\psi^{**}})_l e^{i\mu_l(x_j-a)}, 0 \le j \le M-1, n \ge 0, \tag{3.21}$$

$$\psi_M^n = \psi_0^n,\ \phi_M^n = \phi_0^n,\ n \ge 0. \tag{3.22}$$

where

$$\begin{aligned}(\widetilde{\phi^1})_l &= (\widetilde{\phi^{(0)}})_l \cos(\beta_l k) + \frac{(\widetilde{\phi^{(1)}})_l}{\beta_l}\sin(\beta_l k) + \frac{(1-\cos(\beta_l k))}{\varepsilon^2\beta_l^2}(|\widetilde{\psi^{(0)}}|)_l^2 \\ &+ (\frac{\beta_l k - k\sin(\beta_l k)}{\beta_l^2})(\widetilde{|\psi^{(0)}|^2})_l',\end{aligned} \tag{3.23}$$

$$(\widetilde{\phi^{n+1}})_l = 2(\widetilde{\phi^n})_l \cos(\beta_l k) - (\widetilde{\phi^{n-1}})_l + \frac{2(1-\cos(\beta_l k))}{\varepsilon^2\beta_l^2}(\widetilde{|\psi^n|^2})_l,\ n \ge 1. \tag{3.24}$$

The above EWI-TSFP method for the KGS equations is explicit, uniformly accurate, efficient and can be easily extended to two and three dimensions. The memory cost is $O(M)$ and computational cost is $O(MlnM)$ due to FFT. The numerical results are shown in Section 3.3. We remark here that the EWI method for solving second order wave-type ODEs has been widely used in the literature and it can be tracked back to Gautschi. As is demonstrated in the literature, it gave exact solutions to linear second-order ODEs and showed favorable properties on solving the oscillatory second-order ODEs compared to standard finite difference time discretization. Thus this method will be favorable over ECFD and CNTSFP method for solving the KGS equations in the singular limit regime.

3.2 Another EWI pseudospectral method

Here, we discuss an alternative approach to solving the KG equation efficiently and accurately by using the EWI in temporal discretization and Fourier pseudospectral discretization in space. Similar as EWI method to (2.2), we need to find $\phi_M(x,t), \psi_M(x,t)$ such that

$$\varepsilon^2 \partial_{tt}\phi_M(x,t) - \Delta(\phi_M(x,t)) + \phi_M(x,t) - P_M(|\psi(x,t)|_M^2) = 0. \tag{3.25}$$

Noticing the orthogonality of the Fourier functions, we get the same ODEs with (3.4):

$$\begin{aligned} &\varepsilon^2 \frac{d^2}{dt^2}\widehat{\phi_l(t)} + (\mu_l^2+1)\widehat{\phi_l(t)} - (\widehat{|\psi|^2})_l(t) = 0, \\ &t_n \le t \le t_{n+1},\ n \ge 0,\ l = -\frac{M}{2}, \cdots, \frac{M}{2} - 1. \end{aligned} \tag{3.26}$$

And the general solution for the second-order equation reads

$$\widehat{\phi}_l(t_n+s) = \widehat{\phi}_l(t_n)\cos(\beta_l s) + \widehat{\phi}_l'(t_n)\frac{\sin(\beta_l s)}{\beta_l} + \frac{1}{\varepsilon^2\beta_l}\int_0^s \widehat{f_l^n}(\omega)\sin(\beta_l(s-\omega)d\omega, \tag{3.27}$$

where $\widehat{f_l^n}(\omega) = \widehat{|\psi(t_n+\omega)|^2}_l$. Differentiating (3.27) with respect to s, we obtain

$$\widehat{\phi}_l'(t_n+s) = -\beta_l \sin(\beta_l s)\widehat{\phi}_l(t_n) + \cos(\beta_l s)\widehat{\phi}_l'(t_n) + \frac{1}{\varepsilon^2}\int_0^s \widehat{f_l^n}(\omega)\cos(\beta_l(s-\omega)d\omega. \tag{3.28}$$

Thus, when $n=0$ and $s=k$, from (3.27) and (3.28), we have

$$\widehat{\phi}_l(t_1) = (\widehat{\phi^{(0)}})_l\cos(\beta_l k) + (\widehat{\phi^{(1)}})_l\frac{\sin(\beta_l k)}{\beta_l} + \frac{1}{\varepsilon^2\beta_l}\int_0^k \widehat{f_l^n}(\omega)\sin(\beta_l(k-\omega))d\omega, \tag{3.29}$$

$$\widehat{\phi}_l'(t_1) = -\beta_l \sin(\beta_l k)(\widehat{\phi^{(0)}})_l + \cos(\beta_l k)(\widehat{\phi^{(1)}})_l + \frac{1}{\varepsilon^2}\int_0^k \widehat{f_l^n}(\omega)\cos(\beta_l(k-\omega)d\omega. \tag{3.30}$$

When $n > 0$, setting $s = k$ in (3.27) and (3.28), we get

$$\widehat{\phi}_l(t_{n+1}) = \widehat{\phi}_l(t_n)\cos(\beta_l k) + \widehat{\phi'}_l(t_n)\frac{\sin(\beta_l k)}{\beta_l} + \frac{1}{\varepsilon^2\beta_l}\int_0^k \widehat{f_l^n}(\omega)\sin(\beta_l(k-\omega))d\omega, \tag{3.31}$$

$$\widehat{\phi}'_l(t_{n+1}) = -\beta_l\sin(\beta_l k)\widehat{\phi}_l(t_n) + \cos(\beta_l k)\widehat{\phi'}_l(t_n) + \frac{1}{\varepsilon^2}\int_0^k \widehat{f_l^n}(\omega)\cos(\beta_l(k-\omega)d\omega. \tag{3.32}$$

For the integrations in (3.29)-(3.32), we approximate them as following

$$\begin{aligned}
&\int_0^k \widehat{f_l^n}(\omega)\sin(\beta_l(k-\omega))d\omega = \int_0^k (\widehat{f_l^n}(0) + \omega(\widehat{f_l^n})'(0))\sin(\beta_l(k-\omega)) \\
&\approx \frac{1-\cos(\beta_l k)}{\beta_l}(\widehat{|\psi|^2})_l(t_n) + \frac{\beta_l k - k\sin(\beta_l k)}{\beta_l^2}(\widehat{|\psi|^2})'_l(t_n),
\end{aligned} \tag{3.33}$$

$$\begin{aligned}
&\int_0^k \widehat{f_l^n}(\omega)\cos(\beta_l(k-\omega)d\omega = \int_0^k (\widehat{f_l^n}(0) + \omega(\widehat{f_l^n})'(0))\cos(\beta_l(k-\omega)) \\
&\approx \frac{\sin(\beta_l k)}{\beta_l}(\widehat{|\psi|^2})_l(t_n) + \frac{1-\cos(\beta_l k)}{\beta_l^2}(\widehat{|\psi|^2})'_l(t_n),
\end{aligned} \tag{3.34}$$

where $(\widehat{|\psi|^2})'_l(t_n) \approx ((\widehat{|\psi|^2})_l(t_n) - (\widehat{|\psi|^2})_l(t_{n-1}))/k$ when $n \geq 1$ and $(\widehat{|\psi|^2})'_l(t_0) = (\widehat{|\psi^{(0)}|^2})'_l$, with $(|\psi^{(0)}|^2)' = i(\partial_{xx}\psi^{(0)}\bar{\psi}^{(0)} - \partial_{xx}\bar{\psi}^{(0)}\psi^{(0)})$ thanks to the exact Schrödinger equation.

In practice, we also need to replace the above Fourier spectral approximations by pseudospectral discretization for computational convenience. Choose $\psi_M^0(x)$, $(\phi_M^0)(x)$ and $(\phi_t)_M^0(x)$ as the interpolations of $\psi^{(0)}$, $\phi^{(0)}$ and $\phi^{(1)}$ on the grids, respectively. Let ψ_j^n, ϕ_j^n and $(\phi_t)_j^n$ be the approximations of $\psi(x_j,t_n)$, $\phi(x_j,t_n)$ and $\partial_t\phi(x_j,t_n)$. Denote $\widetilde{\psi}_l(t_n)$, $\widetilde{\phi}_l(t_n)$ and $\widetilde{(\phi_t)}_l(t_n)$ as $(\widetilde{\psi^n})_l$, $(\widetilde{\phi^n})_l$ and $\widetilde{(\phi_t)}_l^n$ which are the discrete pseudospectral coefficients. Combining the split steps via the standard strang splitting, we have the following EWI-TSFP2 scheme:

$$\phi_j^{n+1} = \sum_{l=-\frac{M}{2}}^{\frac{M}{2}-1} (\widetilde{\phi^{n+1}})_l e^{i\mu_l(x_j-a)},\ (\phi_t)_j^{n+1} = \sum_{l=-\frac{M}{2}}^{\frac{M}{2}-1} \widetilde{(\phi_t)}_l^{n+1} e^{i\mu_l(x_j-a)}, \tag{3.35}$$

$$\psi_j^* = \sum_{l=-\frac{M}{2}}^{\frac{M}{2}-1} e^{ik\mu_l^2/2} (\widetilde{\psi^n})_l e^{i\mu_l(x_j-a)}, \tag{3.36}$$

$$\psi_j^{**} = e^{ik(\phi_j^n+\phi_j^{n+1})/2}\psi_j^*, \tag{3.37}$$

$$\psi_j^{n+1} = \sum_{l=-\frac{M}{2}}^{\frac{M}{2}-1} e^{-ik\mu_l^2/2} (\widetilde{\psi^{**}})_l e^{i\mu_l(x_j-a)},\ 0 \le j \le M-1,\ n \ge 0, \tag{3.38}$$

$$\psi_M^n = \psi_0^n,\ \phi_M^n = \phi_0^n,\ n \ge 0, \tag{3.39}$$

where, for $n = 0$,

$$\widetilde{\phi_l^1} = (\widetilde{\phi^{(0)}})_l \cos(\beta_l k) + (\widetilde{\phi^{(1)}})_l \frac{\sin(\beta_l k)}{\beta_l} + \frac{1-\cos(\beta_l k)}{\varepsilon^2\beta_l^2}\widetilde{|\psi^{(0)}|_l^2} + \alpha_l(\widetilde{g})_l, \tag{3.40}$$

$$\widetilde{(\phi_t)}_l^1 = -\beta_l \sin(\beta_l k)(\widetilde{\phi^{(0)}})_l + \cos(\beta_l k)(\widetilde{\phi^{(1)}})_l + \frac{\sin(\beta_l k)}{\varepsilon^2\beta_l}\widetilde{|\psi^{(0)}|_l^2} + \frac{1-\cos(\beta_l k)}{\varepsilon^2\beta_l^2}(\widetilde{g})_l, \tag{3.41}$$

and for $n \ge 1$,

$$(\widetilde{\phi^{n+1}})_l = (\widetilde{\phi^n})_l \cos(\beta_l k) + \widetilde{(\phi_t)^n}_l \frac{\sin(\beta_l k)}{\beta_l} + \frac{1-\cos(\beta_l k)}{\varepsilon^2\beta_l^2}\widetilde{|\psi^n|_l^2} + \alpha_l(\widetilde{\xi^n})_l, \tag{3.42}$$

$$\widetilde{(\phi_t)_l^{n+1}} = -\beta_l \sin(\beta_l k)(\widetilde{\phi^n})_l + \cos(\beta_l)\widetilde{(\phi_t)_l^n} + \frac{\sin(\beta_l k)}{\varepsilon^2\beta_l}\widetilde{|\psi^n|_l^2} + \frac{1-\cos(\beta_l k)}{\varepsilon^2\beta_l^2}(\widetilde{\xi^n})_l, \tag{3.43}$$

with $\alpha_l = \frac{\beta_l k - k\sin(\beta_l k)}{\varepsilon^2\beta_l^3}$, $g = i(\partial_{xx}\psi^{(0)}\bar{\psi}^{(0)} - \partial_{xx}\bar{\psi}^{(0)}\psi^{(0)})$, $\xi^n = \frac{|\psi^n|^2 - |\psi^{n-1}|^2}{k}$ and $(\widetilde{\xi^n})_l$ are the discrete Fourier pseudospectral coefficients of ξ^n defined as

$$(\widetilde{\xi^n})_l = \frac{1}{M}\sum_{j=0}^{M-1} \xi_j^n e^{-i\mu_l(x_j-a)},\ l = -M/2 \cdots M/2-1. \tag{3.44}$$

The initial conditions are discretized as

$$\psi_j^0 = \sum_{l=-M/2}^{M/2-1} (\widetilde{\psi^{(0)}})_l e^{i\mu_l(x_j-a)},\ \phi_j^0 = \sum_{l=-M/2}^{M/2-1} (\widetilde{\phi^{(0)}})_l e^{i\mu_l(x_j-a)},$$

$$(\partial_t\phi)_j^0 = \sum_{l=-M/2}^{M/2-1} (\widetilde{\phi^{(1)}})_l e^{i\mu_l(x_j-a)}.$$

We remark here the above EWI-TSFP2 for solving the KGS equations is very efficient, uniformly accurate and can be easily extended to two and three dimensions. The memory cost is $O(M)$ and computational cost is $O(MlnM)$ due to FFT. The numerical results with the ill-prepared and extremely ill-prepared initial data are given in Section 3.3, which indicates that this method is uniformly accurate.

3.3 Numerical results

In this section, we present the numerical results of the above two EWI-TSFP methods for solving the KGS equations (2.1-2.5) with ill-prepared and extremely ill-prepared initial data. We will show their accuracies for fixed ε and their ε-scalability in the parameter regime when $0 < \varepsilon \ll 1$. The initial data in Example 2 and 3 in the last chapter will be used since finite difference methods and CNTSFP method are not uniformly accurate for these two initial data problems.

Continuing with Example 2 and 3, the initial data in (2.3) are given by (2.103) and (2.106) respectively. The spatial error and temporal error here are computed in a similar way as before. With ill-prepared and extremely ill-prepared initial data, the spatial errors of EWI-TSFP and EWI-TSFP2 are still uniformly accurate. Tabs. 3.1 and 3.2 show the spatial errors of EWI-TSFP and EWI-TSFP2 with the extremely ill-prepared initial data as example, which are uniformly accurate. We omit the spatial error analysis for them with ill-prepared initial data which are very similar with those in Tab. 3.1 and Tab. 3.2.

Tabs. 3.3-3.6 show the temporal errors of EWI-TSFP and EWI-TSFP2 for solving the ill-prepared and extremely ill-prepared initial problem, respectively, under different ε and time step k. Fig. 3.1 and Fig. 3.2 show the temporal error convergence rate, respectively.

From Tabs. 3.1-3.6, we can draw the conclusions (i) EWI-TSFP and EWI-TSFP2 have uniform spectral accuracy in space for all ε (cf. each column in Tabs. 3.1-3.2). The spatial discretization errors are totally independent of ε and the spatial

Table 3.1: Spatial error analysis for $e_{h,k}$ of EWI-TSFP at $T = 2$ with extremely ill-prepared initial data.

EWI-TSFP	$h_0 = 1$	$h_0/2$	$h_0/4$	$h_0/8$
$\varepsilon_0 = 1$	7.06E-2	3.74E-4	2.12E-8	7.06E-12
$\varepsilon_0/2$	8.82E-2	3.61E-4	2.10E-8	7.93E-12
$\varepsilon_0/2^2$	1.02E-1	3.93E-4	2.19E-8	7.72E-12
$\varepsilon_0/2^4$	7.45E-2	6.35E-4	2.38E-8	6.97E-12
$\varepsilon_0/2^6$	7.03E-2	5.74E-4	2.98E-8	1.54E-11
$\varepsilon_0/2^8$	7.30E-2	5.76E-4	2.93E-8	7.50E-12
$\varepsilon_0/2^{10}$	7.28E-2	5.15E-4	2.52E-8	1.17E-11

Table 3.2: Spatial error analysis for $e_{h,k}$ of EWI-TSFP2 at $T = 2$ with extremely ill-prepared initial data.

EWI-TSFP2	$h_0 = 1$	$h_0/2$	$h_0/4$	$h_0/8$
$\varepsilon_0 = 1$	7.06E-2	3.74E-4	2.12E-8	5.32E-12
$\varepsilon_0/2^2$	1.02E-1	3.93E-4	2.19E-8	6.59E-12
$\varepsilon_0/2^4$	7.77E-2	5.49E-4	3.08E-8	1.39E-11
$\varepsilon_0/2^6$	7.59E-2	5.33E-4	3.14E-8	9.08E-12
$\varepsilon_0/2^8$	7.49E-2	4.81E-4	3.16E-8	8.98E-12
$\varepsilon_0/2^{10}$	7.28E-2	5.15E-4	2.52E-8	1.44E-11

resolution is $h = O(1)$, $0 < \varepsilon \ll 1$. (ii) The most important properties of EWI-TSFP and EWI-TSFP2 are that the temporal errors of them are also uniformly accurate for $0 < \varepsilon \ll 1$ with any initial data, which means that the temporal error is totally independent of ε and time resolution is $k = O(1)$. These reach to our main purpose of this thesis. (iii) EWI-TSFP and EWI-TSFP2 have some convergence order reductions or lose the convergence outside the convergence regime (cf. the

Table 3.3: Temporal error analysis for $e_{h,k}$ of EWI-TSFP at $T = 2$ with ill-prepared initial data.

EWI-TSFP	$k_0 = 0.2$	$k_0/2^2$	$k_0/2^4$	$k_0/2^6$	$k_0/2^8$	$k_0/2^9$
$\varepsilon_0 = 1$	1.71E-2	1.06E-3	6.62E-5	4.13E-6	2.54E-7	6.22E-8
$\varepsilon_0/2$	2.55E-2	1.57E-3	9.82E-5	6.13E-6	3.78E-7	9.00E-8
$\varepsilon_0/2^2$	4.20E-2	1.40E-3	8.67E-5	5.41E-6	3.33E-7	7.91E-8
$\varepsilon_0/2^3$	5.86E-2	1.01E-3	6.15E-5	3.84E-6	2.36E-7	5.61E-8
$\varepsilon_0/2^4$	3.52E-1	1.30E-3	5.16E-5	3.21E-6	1.98E-7	4.70E-8
$\varepsilon_0/2^5$	3.39E-1	8.93E-3	5.27E-5	3.26E-6	2.00E-7	4.76E-8
$\varepsilon_0/2^6$	4.42E-1	1.55E-1	6.25E-5	3.18E-6	1.95E-7	4.63E-8
$\varepsilon_0/2^7$	5.33E-1	1.11E-1	4.11E-3	2.94E-6	1.79E-7	4.25E-8
$\varepsilon_0/2^8$	6.64E-1	1.86E-1	1.53E-1	4.44E-6	1.93E-7	4.58E-8
$\varepsilon_0/2^9$	4.99E-1	2.48E-1	1.36E-1	8.67E-4	1.84E-7	4.34E-8
$\varepsilon_0/2^{10}$	4.57E-1	2.97E-1	8.06E-2	7.88E-2	8.77E-7	4.49E-8

very lower diagonal parts in Tabs. 3.3-3.6). However, Fig. 3.1 and Fig. 3.2 show that EWI-TSFP2 has better temporal convergence order than that of EWI-TSFP and thus EWI-TSFP2 is better than EWI-TSFP when $0 < \varepsilon \ll 1$ and EWI-TSFP needs to be improved for optimal convergence.

Table 3.4: Temporal error analysis for $e_{h,k}$ of EWI-TSFP2 at $T = 2$ with ill-prepared initial data.

EWI-TSFP2	$k_0 = 0.2$	$k_0/2^2$	$k_0/2^4$	$k_0/2^6$	$k_0/2^8$	$k_0/2^9$
$\varepsilon_0 = 1$	4.32E-2	2.71E-3	1.69E-4	1.06E-5	6.50E-7	1.54E-7
$\varepsilon_0/2$	9.55E-2	6.54E-3	4.16E-4	2.61E-5	1.60E-6	3.81E-7
$\varepsilon_0/2^2$	6.21E-2	5.05E-3	3.30E-4	2.08E-5	1.28E-6	3.04E-7
$\varepsilon_0/2^3$	6.38E-2	4.92E-3	3.21E-4	2.01E-5	1.24E-6	2.93E-7
$\varepsilon_0/2^4$	2.00E-1	3.63E-3	2.67E-4	1.69E-5	1.04E-6	2.47E-7
$\varepsilon_0/2^5$	1.62E-1	4.80E-3	2.52E-4	1.64E-5	1.01E-6	2.40E-7
$\varepsilon_0/2^6$	2.14E-1	2.86E-2	2.21E-4	1.61E-5	1.00E-6	2.38E-7
$\varepsilon_0/2^7$	2.34E-1	2.12E-2	4.88E-4	1.56E-5	1.00E-6	2.38E-7
$\varepsilon_0/2^8$	2.46E-1	3.51E-2	3.13E-3	1.28E-5	9.78E-7	2.39E-7
$\varepsilon_0/2^9$	2.16E-1	2.75E-2	1.52E-3	4.82E-5	9.28E-7	2.27E-7
$\varepsilon_0/2^{10}$	2.33E-1	3.60E-2	1.74E-3	3.43E-4	8.73E-7	2.42E-7

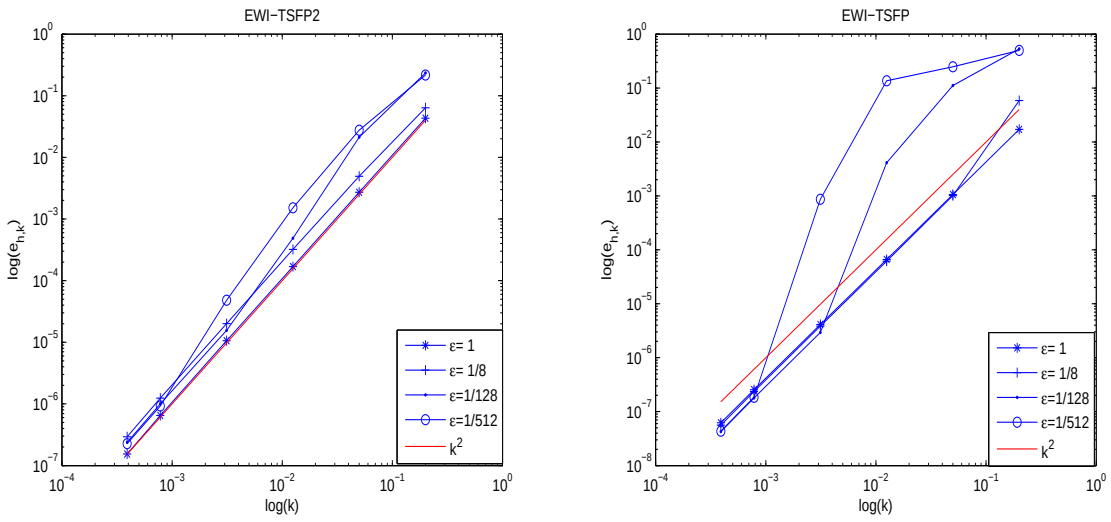

Figure 3.1: Dependence of the temporal errors of EWI-TSFP and EWI-TSFP2 on k at $t = 2$ with difference ε for the ill-prepared initial problem.

Table 3.5: Temporal error analysis for $e_{h,k}$ of EWI-TSFP at $T = 2$ with extremely ill-prepared initial data.

EWI-TSFP	$k_0 = 0.2$	$k_0/4$	$k_0/2^4$	$k_0/2^6$	$k_0/2^8$	$k_0/2^9$
$\varepsilon_0 = 1$	1.71E-2	1.06E-3	6.62E-05	4.13E-6	2.54E-7	6.22E-8
$\varepsilon_0/2$	3.06E-2	1.90E-3	1.18E-4	7.39E-6	4.56E-7	1.09E-7
$\varepsilon_0/2^2$	5.21E-2	2.44E-3	1.53E-4	9.54E-6	5.87E-7	1.40E-7
$\varepsilon_0/2^3$	5.75E-2	1.53E-3	9.51E-5	5.94E-6	3.65E-7	8.68E-8
$\varepsilon_0/2^4$	3.62E-1	2.13E-3	1.12E-4	7.00E-6	4.31E-7	1.02E-7
$\varepsilon_0/2^5$	6.93E-1	1.03E-2	1.47E-4	9.14E-6	5.62E-7	1.33E-7
$\varepsilon_0/2^6$	4.99E-1	1.60E-1	9.46E-5	5.47E-6	3.37E-7	8.00E-8
$\varepsilon_0/2^7$	5.55E-1	1.29E-1	4.22E-3	9.63E-6	5.90E-7	1.40E-7
$\varepsilon_0/2^8$	6.16E-1	1.98E-1	7.49E-2	1.53E-5	6.78E-7	1.61E-7
$\varepsilon_0/2^9$	6.45E-1	2.56E-1	5.57E-2	2.04E-3	1.02E-6	2.41E-7

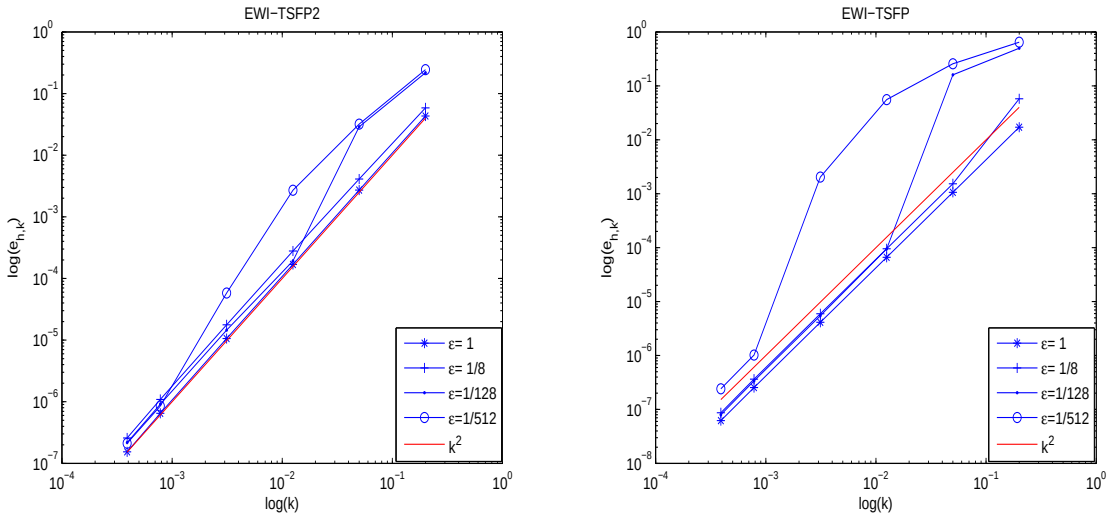

Figure 3.2: Dependence of the temporal errors of EWI-TSFP and EWI-TSFP2 on k at $t = 2$ with difference ε for the extremely ill-prepared initial problem.

Table 3.6: Temporal error analysis for $e_{h,k}$ of EWI-TSFP2 at $T = 2$ with extremely ill-prepared initial data.

EWI-TSFP2	$k_0 = 0.2$	$k_0/4$	$k_0/2^4$	$k_0/2^6$	$k_0/2^8$	$k_0/2^9$
$\varepsilon_0 = 1$	4.32E-2	2.71E-3	1.69E-4	1.06E-5	6.50E-7	1.54E-7
$\varepsilon_0/2$	1.03E-1	7.20E-3	4.59E-4	2.88E-5	1.77E-6	4.21E-7
$\varepsilon_0/2^2$	6.91E-2	5.99E-3	3.92E-4	2.47E-5	1.52E-6	3.61E-7
$\varepsilon_0/2^3$	5.86E-2	4.11E-3	2.79E-4	1.77E-5	1.09E-6	2.59E-7
$\varepsilon_0/2^4$	2.02E-1	3.05E-3	2.33E-4	1.50E-5	9.25E-7	2.20E-7
$\varepsilon_0/2^5$	1.66E-1	4.75E-3	2.22E-4	1.48E-5	9.20E-7	2.19E-7
$\varepsilon_0/2^6$	2.18E-1	2.89E-2	1.92E-4	1.45E-5	9.14E-7	2.18E-7
$\varepsilon_0/2^7$	2.39E-1	2.16E-2	4.87E-4	1.38E-5	9.07E-7	2.17E-7
$\varepsilon_0/2^8$	2.43E-1	2.93E-2	3.69E-3	1.20E-5	8.91E-7	2.15E-7
$\varepsilon_0/2^9$	2.44E-1	3.19E-2	2.70E-3	5.80E-5	8.50E-7	2.12E-7

Chapter 4

Uniform and optimal numerical methods

In this chapter, we are going to propose two multiscale methods based on the multiscale analysis of the KGS equations. Multiscale analysis is widely used to construct uniformly valid approximations to the solutions of perturbation problems, for small values of the parameter involved in the problem. It is done by introducing fast-scale and slow-scale variables for an independent variable, and subsequently treating these variables, fast and slow, as if they are independent [48]. We propose the multiscale analysis of the KGS equations in order to know the osscillation properties of the solutions to the KGS equations theoretically under three main types of initial conditions. Two multiscale methods are designed with the application of EWI-TSFP and EWI-TSFP2 methods for the decomposed KGS equations.

4.1 Multiscale analysis

In this section, we will apply the multiscale method to generalized KGS equations (2.1)-(2.3) in singular limit regime. Let $\tau = t/\varepsilon$ be the fast time variable, and here we present two-scale matched asymptotic expansion. Using the standard perturbations

analysis, we extend $\psi(x,t)$ and $\phi(x,t)$ as

$$\psi(x,t) = \psi_0(x,t) + \varepsilon\psi_1^f(x,\tau) + \varepsilon\psi_1(x,t) + \cdots, \tag{4.1}$$

$$\phi(x,t) = \phi_0(x,t) + \phi_0^f(x,\tau) + \varepsilon\phi_1(x,t) + \varepsilon\phi_1^f(x,\tau) + \cdots. \tag{4.2}$$

Plugging the (4.1) and (4.2) into the generalized KGS equations (2.1), (2.2) and the initial conditions (2.3), we can get

$$\begin{aligned}&[i\partial_t\psi_0 + \Delta\psi_0 + \phi_0\psi_0](x,t) + [i\partial_\tau\psi_1^f + \psi_0\phi_0^f](x,\tau)\\ &+ \varepsilon[i\partial_t\psi_1 + \Delta\psi_1 + \psi_0\phi_1 + \psi_1\phi_0] + \cdots = 0,\end{aligned} \tag{4.3}$$

$$\begin{aligned}&[-\Delta\phi_0 + \phi_0 - |\psi_0|^2] + [\partial_{\tau\tau}\phi_0^f - \Delta\phi_0^f + \phi_0^f]\\ &+ \varepsilon[-\Delta\phi_1 + \phi_1 - (\psi_1(x,t)\bar{\psi}_0(x,t) + \psi_0(x,t)\bar{\psi}_1(x,t))]\\ &+ \varepsilon[\partial_{\tau\tau}\phi_1^f - \Delta\phi_1^f + \phi_1^f - 2Re(\psi_0(x,t)\bar{\psi}_1^f)(x,\tau)] + \cdots = 0,\end{aligned} \tag{4.4}$$

with the initial conditions

$$\begin{aligned}&\psi(x,0) = \psi_0(x,0) + \varepsilon\psi_1^f(x,0) + \varepsilon\psi_1(x,0) + \cdots,\\ &\phi(x,0) = \phi_0(x,0) + \phi_0^f(x,0) + \varepsilon\phi_1(x,0) + \varepsilon\phi_1^f(x,0) + \cdots,\\ &\partial_t\phi(x,0) = \partial_t\phi_0(x,0) + \frac{1}{\varepsilon}\partial_\tau\phi_0^f(x,0) + \varepsilon\partial_t\phi_1(x,0) + \partial_\tau\phi_1^f(x,0) + \cdots.\end{aligned} \tag{4.5}$$

By the asymptotic analysis principles, the form of the solutions $\psi(x,t)$ and $\phi(x,t)$ depend on different initial conditions. Suppose that the initial data are

$$\psi(x,0) = \psi^{(0)}(x), \tag{4.6}$$

$$\phi(x,0) = \phi^{(0)}(x) = \phi_0(x,0) + \varepsilon^\alpha w_1(x), \tag{4.7}$$

$$\partial_t\phi(x,0) = \phi^{(1)}(x) = \partial_t\phi_0(x,0) + \varepsilon^\beta w_2(x), \tag{4.8}$$

where $\phi_0(x,0) = (-\Delta + I)^{-1}|\psi^{(0)}|^2$ and $\partial_t\phi_0(x,0) = -i(-\Delta + I)^{-1}\nabla\cdot(\psi^{(0)}\nabla\bar{\psi}^{(0)} - \bar{\psi}^{(0)}\nabla\psi^{(0)})$; α and β are nonnegative integers; $w_1(x)$ and $w_2(x)$ are uniformly bounded in H^2 w.r.t. ε. Assuming $\psi^{(0)}(x)$ is the initial of the SY equations, then $\phi_0(x,0)$

and $\partial_t\phi_0(x,0)$ are deducted from the SY equations:

$$i\partial_t\psi_0(x,t)+\Delta\psi_0(x,t)+\phi_0(x,t)\psi_0(x,t)=0, \tag{4.9}$$

$$-\Delta\phi_0(x,t)+\phi_0(x,t)-|\psi_0(x,t)|^2=0, \tag{4.10}$$

$$\psi_0(x,0)=\psi^{(0)}(x). \tag{4.11}$$

Here we mainly state three cases.

Case 1. When $\alpha\geq 2$ and $\beta\geq 1$, the initial data are the so-called well-prepared initial data and we can derive from the system (4.3)-(4.5) to get

$$\psi(x,t)=\psi_0(x,t)+\varepsilon\psi_1(x,t)+\varepsilon^3\psi_3^f(x,\tau)+\cdots, \tag{4.12}$$

$$\phi(x,t)=\phi_0(x,t)+\varepsilon\phi_1(x,t)+\varepsilon^2\phi_2^f(x,\tau)+\cdots, \tag{4.13}$$

where $\psi_0(x,t)$ and $\phi_0(x,t)$ satisfies the SY equations (4.9)-(4.11); $\psi_1(x,t)$ and $\phi_1(x,t)$ satisfy

$$i\partial_t\psi_1(x,t)+\Delta\psi_1(x,t)+\phi_0(x,t)\psi_1(x,t)+\phi_1(x,t)\psi_0(x,t)=0, \tag{4.14}$$

$$-\Delta\phi_1(x,t)+\phi_1(x,t)-Re(\psi_1(x,t)\bar{\psi}_0(x,t)+\psi_0(x,t)\bar{\psi}_1(x,t))=0, \tag{4.15}$$

$$\psi_1(x,0)=0. \tag{4.16}$$

Case 2. When $\alpha\geq 1$ and $\beta=0$, we have $\phi_0^f(x,\tau)=0$ and the asymptotic expansions are in the form of

$$\psi(x,t)=\psi_0(x,t)+\varepsilon\psi_1(x,t)+\varepsilon^2\psi_2^f(x,\tau)+\cdots, \tag{4.17}$$

$$\phi(x,t)=\phi_0(x,t)+\varepsilon\phi_1(x,t)+\varepsilon\phi_1^f(x,\tau)+\cdots. \tag{4.18}$$

where $\psi_0(x,t)$ and $\phi_0(x,t)$ satisfy the SY equations (4.9)-(4.11); $\psi_1(x,t)$ and $\phi_1(x,t)$ also satisfy (4.14)-(4.16); $\phi_1^f(x,\tau)$ and $\psi_2^f(x,\tau)$ satisfy

$$i\partial_\tau\psi_2^f(x,\tau)+\psi_0(x,t)\phi_1^f(x,\tau)=0, \tag{4.19}$$

$$\psi_2^f(x,0)=0, \tag{4.20}$$

$$\partial_{\tau\tau}\phi_1^f(x,\tau) - \Delta\phi_1^f(x,\tau) + \phi_1^f(x,\tau) = 0,$$
$$\phi_1^f(x,0) = w_1(x)(e.g.\ \alpha = 1)\ or\ \phi_1^f(x,0) = 0\ (e.g.\ \alpha > 1),\ \partial_\tau\phi_1^f = w_2(x). \tag{4.21}$$

and ϕ_1^f can be solved exactly.

Case 3. When $\alpha = 0$ and $\beta \geq 0$, i.e., the extremely ill-prepared initial data, the asymptotic solutions are give by (4.1) and (4.2), in which $\psi_0(x,t)$, $\phi_0(x,t)$, $\psi_1(x,t)$ and $\phi_1(x,t)$ satisfy (4.9)-(4.11) and (4.14)-(4.16) respectively; $\psi_1^f(x,\tau)$ and $\phi_0^f(x,\tau)$ satisfy

$$i\partial_\tau\psi_1^f(x,\tau) + \psi_0(x,t)\phi_0^f(x,\tau) = 0, \tag{4.22}$$
$$\psi_1^f(x,0) = 0, \tag{4.23}$$

and

$$\partial_{\tau\tau}\phi_0^f(x,\tau) - \Delta\phi_0^f(x,\tau) + \phi_0^f(x,\tau) = 0, \tag{4.24}$$
$$\phi_0^f(x,0) = w_1(x),\ \phi_0^f(x,0) = 0. \tag{4.25}$$

It is easy to know that $\phi_0^f(x,\tau)$ can be solved out exactly. What's more, $\phi_1^f(x,\tau)$ satisfies

$$\partial_{\tau\tau}\phi_1^f(x,\tau) - \Delta\phi_1^f(x,\tau) + \phi_1^f(x,\tau) - 2Re(\psi_0(x,t)\bar{\psi}_1^f(x,\tau)) = 0, \tag{4.26}$$
$$\phi_1^f(x,0) = -\phi_1(x,0),\ \partial_\tau\phi_1^f = w_2(x),\ (e.g.\beta = 0)\ or\ \partial_\tau\phi_1^f = 0. \tag{4.27}$$

4.2 Multiscale methods

We firstly focus on Case 2 as an example. The main oscillatory term of the solution $\phi(x,t)$ which contains the fast variable is $\phi_1^f(x,\tau)$. It satisfies the linear Klein-Gordon equation (4.21). By using Fourier spectral method, we can get the exact solution to ϕ_1^f with proper initial data, which is our starting point of designing new methods. Again, denote $X_M := span\left\{e^{i\mu_l(x-a)},\ \mu_l = \frac{2\pi l}{b-a},\ l = \frac{-M}{2}\cdots\frac{M}{2}-1\right\}$, $Y_M := span\left\{v = (v_0, v_1, \cdots, v_M),\ v_0 = v_M\right\}$. For a general periodic function $v(x)$

on $[a,b]$ and a vector a vector $v \in Y_M$, let $P_M : L^2([a,b]) \to X_M$ be the standard L^2-projection operator onto X_M, $I_M : Y_M \to X_M$ be the trigonometric interpolation operator:

$$(P_M v)(x) = \sum_{l=-M/2}^{M/2-1} \widehat{v}_l e^{i\mu_l(x-a)}, \ (I_M v)(x) = \sum_{l=-M/2}^{M/2-1} \widetilde{v}_l e^{i\mu_l(x-a)}, \ a \le x \le b, \tag{4.28}$$

where

$$\widehat{v}_l = \frac{1}{b-a}\int_a^b v(x) e^{-i\mu_l(x-a)}, \quad \widetilde{v}_l = \frac{1}{M}\sum_{j=0}^{M-1} v_j e^{-i\mu_l(x_j-a)}, \tag{4.29}$$

with v_j interpreted as $v(x_j)$ for a function $v(x)$.

Let us continue with the KGS equations (2.1)-(2.5) with the following initial conditions as example

$$\psi(x,0) = \psi^{(0)}(x), \tag{4.30}$$

$$\phi(x,0) = \phi^{(0)}(x) = \phi_0(x) + \varepsilon w_1(x), \tag{4.31}$$

$$\partial_t \phi(x,0) = \phi^{(1)}(x) = \phi_1(x) + w_2(x), \tag{4.32}$$

where $\phi_0(x) = (-\Delta + I)^{-1}|\psi^{(0)}|^2$ and $\phi_1(x) = -i(-\Delta + I)^{-1}\nabla \cdot (\psi^{(0)}\nabla\bar{\psi}^{(0)} - \bar{\psi}^{(0)}\nabla\psi^{(0)})$; $w_1(x)$ and $w_2(x)$ are uniformly bounded in H^2 w.r.t. ε. Based on the multiscale analysis, let $\phi(x,t) = \phi^{\varepsilon}(x,t) + \varepsilon\phi_1^f(x,\tau)$ and we can get $\phi^{\varepsilon}(x,t)$ and $\phi^f(x,\tau)$ are satisfying

$$\begin{aligned} &\varepsilon^2\partial_{tt}\phi^{\varepsilon} - \Delta\phi^{\varepsilon} + \phi^{\varepsilon} - |\psi|^2 = 0, \ a < x < b, \ t > 0, \\ &\phi^{\varepsilon}(x,0) = \phi_0(x), \ \partial_t\phi^{\varepsilon} = \phi_1(x), \end{aligned} \tag{4.33}$$

$$\begin{aligned} &\partial_{\tau\tau}\phi_1^f(x,\tau) - \Delta\phi_1^f(x,\tau) + \phi_1^f(x,\tau) = 0, \ a < x < b, \ \tau > 0, \\ &\phi_1^f(x,0) = w_1(x), \ \partial_\tau\phi_1^f = w_2(x), \end{aligned} \tag{4.34}$$

where the equation in (4.33) is the Klein-Gordon equation which can be solved by the EWI method with periodic boundaries shown in the beginning of Section 3.1. And the equation in (4.34) can be solve exactly as the following:

Applying P_M on the equation (4.34), and noticing the orthogonality of the Fourier functions, we get the the ODEs:

$$\varepsilon^2 \frac{d^2}{d\tau^2} \widehat{(\phi_1^f)}_l(\tau) + (\mu_l^2 + 1) \widehat{(\phi_1^f)}_l(\tau) = 0. \tag{4.35}$$

It is easy to get the solution to this ODEs with proper initial data. Thus

$$\begin{aligned} \phi_1^f(x,\tau) &= \sum_{l=-M/2}^{M/2-1} \widehat{(\phi_1^f)}_l e^{i\mu_l(x-a)} \\ &= \sum_{l=-M/2}^{M/2-1} \left((\widehat{w_1})_l \cos(\gamma_l \tau) + (\widehat{w_2})_l \frac{\sin(\gamma_l \tau)}{\gamma_l} \right) e^{i\mu_l(x-a)}, \end{aligned} \tag{4.36}$$

where $\gamma_l = \sqrt{\mu_l^2 + 1}/2$ and $\tau = t/\varepsilon$. Then the integration of $\phi_1^f(x,\tau)$ with respect to t from t_n to t_{n+1} is given by

$$\begin{aligned} \int_{t_n}^{t_{n+1}} \phi_1^f(x, t/\varepsilon) dt = \sum_{l=-M/2}^{M/2-1} \Bigg[& \frac{\varepsilon}{\gamma_l} \left(\sin\left(\frac{\gamma_l t_{n+1}}{\varepsilon}\right) - \sin\left(\frac{\gamma_l t_n}{\varepsilon}\right) \right) (\widehat{w_1})_l e^{i\mu_l(x-a)} \\ & - \frac{\varepsilon}{\gamma_l^2} \left(\cos\left(\frac{\gamma_l t_{n+1}}{\varepsilon}\right) - \cos\left(\frac{\gamma_l t_n}{\varepsilon}\right) \right) (\widehat{w_2})_l e^{i\mu_l(x-a)} \Bigg]. \end{aligned} \tag{4.37}$$

Then we can improve the time-splitting method for solving the NLSE in the KGS equations with separation of $\phi(x,t)$ with high perturbation term and slow perturbation term.

From time $t = t_n$ to $t = t_{n+1}$, the Schrödinger equation (2.1) is solved in two splitting steps which we stated in Chapter 2. For the second step, we can rewrite the equation as

$$i\partial_t \psi + \phi^\varepsilon \psi + \varepsilon \phi_1^f \psi = 0, \ t_n \le t \le t_{n+1}. \tag{4.38}$$

Integrating (4.38) from $t = t_n$ to t_{n+1}, and approximating the integral of slow perturbation term $\phi^\varepsilon(x,t) = \phi(x,t) - \varepsilon\phi_1^f(x,\tau)$ on $[t_n, t_{n+1}]$ via the trapezoidal rule, one obtains

$$\psi(x, t_{n+1}) \approx e^{\frac{ik}{2}[\phi^\varepsilon(x,t_n) + \phi^\varepsilon(x,t_{n+1})]} e^{\int_{t_n}^{t_{n+1}} \varepsilon\phi_1^f(x,t/\varepsilon)dt} \psi(x,t_n), \ a \le x \le b. \tag{4.39}$$

where $e^{\int_{t_n}^{t_{n+1}} \varepsilon\phi_1^f(x,t/\varepsilon)dt}$ can be given exactly.

Note that the error in the numerical integration via the trapezoidal rule depends on the second order partial derivatives of $\phi^\varepsilon(x,t)$ w.r.t. t, which is uniformly bounded to ε. From this point of view, we can improve the time-splitting method for solving the Schrödinger equation. By coupling it with the EWI method for solving the Klein-Gordon equation (4.33) and the Fourier spectral exact solution (4.36), we can get the multiscale methods.

Again, due to the difficulty in calculations of the integrals defining the Fourier transform coefficients, we adopt an efficient implementation by choosing $\psi^0(x)$, $(\phi^0)(x)$ and $(\phi_t)^0(x)$ as the interpolations of $\psi^{(0)}$, $\phi^{(0)}$ and $\phi^{(1)}$ on the grids, respectively. Let ψ_j^n and ϕ_j^n be the approximations of $\psi(x_j,t_n)$ and $\phi(x_j,t_n)$. $(\phi_1^f)_j^n$ is interpreted as $(\phi_1^f)(x_j,\frac{t_n}{\varepsilon})$. Then the multiscale EWI-TSFP method reads

$$\phi_j^{n+1} = (\phi^\varepsilon)_j^{n+1} + \varepsilon(\phi_1^f)_j^{n+1}, \tag{4.40}$$

$$(\phi^\varepsilon)_j^{n+1} = \sum_{l=-\frac{M}{2}}^{\frac{M}{2}-1} (\widetilde{\phi_\varepsilon^{n+1}})_l e^{i\mu_l(x_j-a)}, \tag{4.41}$$

$$(\phi_1^f)_j^{n+1} = \sum_{l=-M/2}^{M/2-1} \Big((\widetilde{w_1})_l \cos(\gamma_l t_{n+1}/\varepsilon) + (\widetilde{w_2})_l \frac{\sin(\gamma_l t_{n+1}/\varepsilon)}{\gamma_l} \Big) e^{i\mu_l(x_j-a)}, \tag{4.42}$$

$$\psi_j^* = \sum_{l=-\frac{M}{2}}^{\frac{M}{2}-1} e^{ik\mu_l^2/2} (\widetilde{\psi^n})_l e^{i\mu_l(x_j-a)}, \tag{4.43}$$

$$\psi_j^{**} = e^{ik((\phi^\varepsilon)_j^n + (\phi^\varepsilon)_j^{n+1})/2} E_j^n \psi_j^*, \tag{4.44}$$

$$\psi_j^{n+1} = \sum_{l=-\frac{M}{2}}^{\frac{M}{2}-1} e^{-ik\mu_l^2/2} (\widetilde{\psi^{**}})_l e^{i\mu_l(x_j-a)}, \ 0 \le j \le M-1, \tag{4.45}$$

$$\psi_M^n = \psi_0^n, \ \phi_M^n = \phi_0^n, \ n \ge 0, \tag{4.46}$$

where

$$
\begin{aligned}
(\widetilde{\phi}_\varepsilon^1)_l &= (\widetilde{\phi}_0)_l \cos(\beta_l k) + \frac{(\widetilde{\phi}_1)_l}{\beta_l}\sin(\beta_l k) + \frac{(1-\cos(\beta_l k))}{\varepsilon^2\beta_l^2}\widetilde{(|\psi^{(0)}|^2)}_l \\
&+ (\frac{\beta_l k - k\sin(\beta_l k)}{\varepsilon^2\beta_l^3})\widetilde{g}_l,
\end{aligned} \tag{4.47}
$$

$$
(\widetilde{\phi_\varepsilon^{n+1}})_l = 2(\widetilde{\phi_\varepsilon^n})_l \cos(\beta_l k) - (\widetilde{\phi_\varepsilon^{n-1}})_l + \frac{2(1-\cos(\beta_l k))}{\varepsilon^2\beta_l^2}(\widetilde{|\psi^n|^2})_l,\ n \geq 1, \tag{4.48}
$$

with $g = i(\partial_{xx}\psi^{(0)}\bar{\psi}^{(0)} - \partial_{xx}\bar{\psi}^{(0)}\psi^{(0)})$, and

$$
E_j^n = e^{f_j^n}, \tag{4.49}
$$

with

$$
\begin{aligned}
f_j^n = \varepsilon \sum_{l=-M/2}^{M/2-1} \Bigg[&\frac{\varepsilon}{\gamma_l}\left(\sin\left(\frac{\gamma_l t_{n+1}}{\varepsilon}\right) - \sin\left(\frac{\gamma_l t_n}{\varepsilon}\right)\right)(\widehat{w_1})_l e^{i\mu_l(x_j-a)} \\
&- \frac{\varepsilon}{\gamma_l^2}\left(\cos\left(\frac{\gamma_l t_{n+1}}{\varepsilon}\right) - \cos\left(\frac{\gamma_l t_n}{\varepsilon}\right)\right)(\widehat{w_2})_l e^{i\mu_l(x_j-a)}\Bigg].
\end{aligned} \tag{4.50}
$$

The initial conditions are discretized as

$$
\begin{aligned}
&\psi_j^0 = \sum_{l=-M/2}^{M/2-1} \widetilde{(\psi^{(0)})}_l e^{i\mu_l(x_j-a)},\ (\phi^\varepsilon)_j^0 = \sum_{l=-M/2}^{M/2-1} (\widetilde{\phi}_0)_l e^{i\mu_l(x_j-a)}, \\
&(\partial_t\phi^\varepsilon)_j^0 = \sum_{l=-M/2}^{M/2-1} (\widetilde{\phi}_1)_l e^{i\mu_l(x_j-a)},\ (\phi_1^f)_j^0 = \sum_{l=-M/2}^{M/2-1} (\widetilde{w_1})_l e^{i\mu_l(x_j-a)}, \\
&(\partial_\tau\phi_1^f)_j^0 = \sum_{l=-M/2}^{M/2-1} (\widetilde{w_2})_l e^{i\mu_l(x_j-a)},
\end{aligned}
$$

where $(\widetilde{v})_l$ $(l = -M/2\cdots M/2-1)$ are the discrete Fourier pseudospectral coefficients of the vector $v = (v_0,\ v_1, \cdots v_M) \in Y_M$ defined as

$$
(\widetilde{v})_l = \frac{1}{M}\sum_{j=0}^{M-1} v_j e^{-i\mu_l(x_j-a)},\ l = -M/2\cdots M/2-1. \tag{4.51}
$$

This multiscale EWI-TSFP method is explicit, uniformly accurate, easy to implement and very efficient due to the fast Fourier transform (FFT), and its memory cost is $O(M)$ and the computational cost per time step is $O(MlnM)$.

Similarly, we can propose the multiscale EWI-TSFP2 scheme as following:

$$\phi_j^{n+1} = (\phi^{\varepsilon})_j^{n+1} + \varepsilon(\phi_1^f)_j^{n+1}, \tag{4.52}$$

$$(\phi^{\varepsilon})_j^{n+1} = \sum_{l=-\frac{M}{2}}^{\frac{M}{2}-1} (\widetilde{\phi_{\varepsilon}^{n+1}})_l e^{i\mu_l(x_j-a)}, \ (\phi_t^{\varepsilon})_j^{n+1} = \sum_{l=-\frac{M}{2}}^{\frac{M}{2}-1} \widetilde{(\phi_t^{\varepsilon})}_l^{n+1} e^{i\mu_l(x_j-a)}, \tag{4.53}$$

$$(\phi_1^f)_j^n = \sum_{l=-M/2}^{M/2-1} \Big((\widetilde{w_1})_l \cos(\gamma_l t_n/\varepsilon) + (\widetilde{w_2})_l \frac{\sin(\gamma_l t_n/\varepsilon)}{\gamma_l} \Big) e^{i\mu_l(x_j-a)}, \tag{4.54}$$

$$\psi_j^* = \sum_{l=-\frac{M}{2}}^{\frac{M}{2}-1} e^{ik\mu_l^2/2} (\widetilde{\psi}^n)_l e^{i\mu_l(x_j-a)}, \tag{4.55}$$

$$\psi_j^{**} = e^{ik(\phi_j^n+\phi_j^{n+1})/2}\psi_j^*, \tag{4.56}$$

$$\psi_j^{n+1} = \sum_{l=-\frac{M}{2}}^{\frac{M}{2}-1} e^{-ik\mu_l^2/2} (\widetilde{\psi^{**}})_l e^{i\mu_l(x_j-a)}, \ 0 \le j \le M-1, n \ge 0, \tag{4.57}$$

$$\psi_M^n = \psi_0^n, \ \phi_M^n = \phi_0^n, \ n \ge 0, \tag{4.58}$$

where, E_j^n is given in (4.49); for $n = 0$,

$$(\widetilde{\phi_{\varepsilon}^1})_l = (\widetilde{\phi_0})_l \cos(\beta_l k) + (\widetilde{\phi_1})_l \frac{\sin(\beta_l k)}{\beta_l} + \frac{1-\cos(\beta_l k)}{\varepsilon^2\beta_l^2} \widetilde{|\psi^{(0)}|_l^2} + \alpha_l \widetilde{g}_l, \tag{4.59}$$

$$\widetilde{(\phi_t^{\varepsilon})}_l^1 = -\beta_l \sin(\beta_l k)(\widetilde{\phi_0})_l + \cos(\beta_l k)(\widetilde{\phi_1})_l + \frac{\sin(\beta_l k)}{\varepsilon^2\beta_l} \widetilde{|\psi^{(0)}|_l^2} + \frac{1-\cos(\beta_l k)}{\varepsilon^2\beta_l^2} \widetilde{g}_l, \tag{4.60}$$

and for $n \ge 1$,

$$(\widetilde{\phi_{\varepsilon}^{n+1}})_l = (\widetilde{\phi_{\varepsilon}^n})_l \cos(\beta_l k) + \widetilde{(\phi_t^{\varepsilon})_l^n} \frac{\sin(\beta_l k)}{\beta_l} + \frac{1-\cos(\beta_l k)}{\varepsilon^2\beta_l^2} \widetilde{|\psi^n|_l^2} + \alpha_l \widetilde{\xi}_l^n, \tag{4.61}$$

$$\widetilde{(\phi_t^{\varepsilon})_l^{n+1}} = -\beta_l \sin(\beta_l k)(\widetilde{\phi_{\varepsilon}^n})_l + \cos(\beta_l)\widetilde{(\phi_t^{\varepsilon})_l^n} + \frac{\sin(\beta_l k)}{\varepsilon^2\beta_l} \widetilde{|\psi^n|_l^2} + \frac{1-\cos(\beta_l k)}{\varepsilon^2\beta_l^2} \widetilde{\xi}_l^n, \tag{4.62}$$

with $\alpha_l = \frac{\beta_l k - k\sin(\beta_l k)}{\varepsilon^2\beta_l^3}$, $g = i(\partial_{xx}\psi^{(0)}\bar{\psi}^{(0)} - \partial_{xx}\bar{\psi}^{(0)}\psi^{(0)})$, $\xi^n = \frac{|\psi^n|^2 - |\psi^{n-1}|^2}{k}$ and $\widetilde{\xi}_l^n$ are the discrete Fourier pseudospectral coefficients of ξ^n defined as

$$\widetilde{\xi^n}_l = \frac{1}{M} \sum_{j=0}^{M-1} \xi_j^n e^{-i\mu_l(x_j-a)}, \ l = -M/2 \cdots M/2 - 1. \tag{4.63}$$

Remark 4.2.1. *These multiscale methods are only suitable for solving the KGS equations with certain kind of initial data. Once the type of the initial condition is changed to other types, the multiscale asymptotic decomposition will be changed.*

Remark 4.2.2. *The numerical methods for solving KGS with extremely ill-prepared initial data shown in Case 3 can be solved with the similar skills. For example, let* $\phi(x,t) = \phi^{\varepsilon}(x,t) + \phi_0^f(x,\tau) + \varepsilon\phi_1^f(x,\tau)$, *where* $\phi^{\varepsilon}(x,t)$ *satisfies (4.33) and* $\phi_0^f(x,\tau)$, $\phi_1^f(x,\tau)$ *can be solved exactly with proper initial data, we can proposed the multiscale methods similarly.*

4.3 Numerical results

In this section, we continue with example 2, an example of ill-prepared data in Section 2.3. We will show their accuracy for fixed ε and their ε-scalability in the parameter regime when $0 < \varepsilon \ll 1$. With the definition of error in (2.102), the spatial and temporal error analysis here are computed in a similar way as before. Tabs. 4.1-4.2 show the temporal error analysis of these two multiscale methods with example 2. Tab. 4.3 shows the spatial error of MEWI-TSFP method with different ε and k, which indicates that MEWI-TSFP for solving ill-prepared initial problem has uniform and optimal spectral accuracy. The MEWI-TSFP2 shows very similar spatial errors with those of MEWI-TSFP, thus we omit them for brevity. In order to know the temporal error convergence order, we plot the dependence of the temporal errors on k under different ε in Fig. 4.1.

From Tabs. 4.1-4.3, we can draw the conclusion that the multiscale methods designed specially for ill-prepared initial problem have uniformly spectral accuracy in space and uniform accuracy in time. The ε-scalability is $h = O(1)$ and $k = O(1)$ for all $0 < \varepsilon \leq 1$. Fig. 4.1 shows these two methods have almost second-order accuracy in time. Compared with the numerical results of EWI-TSFP method in Tab. 3.3, Tab. 4.1 shows that the multiscale EWI-TSFP method has much improved on the temporal accuracy when ε is sufficiently small.

Table 4.1: Temporal error analysis for $e_{h,k}$ of MEWI-TSFP at $T = 2$ with ill-prepared initial data.

MEWI-TSFP	$k_0 = 0.2$	$k_0/4$	$k_0/2^4$	$k_0/2^6$	$k_0/2^8$	$k_0/2^9$
$\varepsilon_0 = 1$	2.83E-1	1.96E-2	1.25E-3	7.85E-5	4.84E-6	1.15E-6
$\varepsilon_0/2$	1.43E-1	9.83E-3	6.27E-4	3.93E-5	2.42E-6	5.75E-7
$\varepsilon_0/2^2$	1.24E-1	8.13E-3	5.09E-4	3.18E-5	1.95E-6	4.64E-7
$\varepsilon_0/2^3$	1.09E-1	1.04E-2	6.72E-4	4.20E-5	2.59E-6	6.14E-7
$\varepsilon_0/2^4$	1.46E-1	1.19E-2	7.41E-4	4.50E-5	2.74E-6	6.51E-7
$\varepsilon_0/2^5$	1.26E-1	1.33E-2	7.54E-4	4.34E-5	2.62E-6	6.21E-7
$\varepsilon_0/2^6$	1.51E-1	1.82E-2	8.23E-4	6.48E-5	4.16E-6	9.95E-7
$\varepsilon_0/2^7$	1.65E-1	1.32E-2	1.14E-3	5.91E-5	3.73E-06	8.95E-7
$\varepsilon_0/2^8$	1.76E-1	2.12E-2	1.85E-3	9.83E-5	6.76E-6	1.61E-6
$\varepsilon_0/2^9$	1.56E-1	1.70E-2	9.45E-4	9.09E-5	8.53E-6	2.13E-6
$\varepsilon_0/2^{10}$	1.66E-1	2.32E-2	1.05E-3	2.19E-4	1.31E-5	3.37E-6

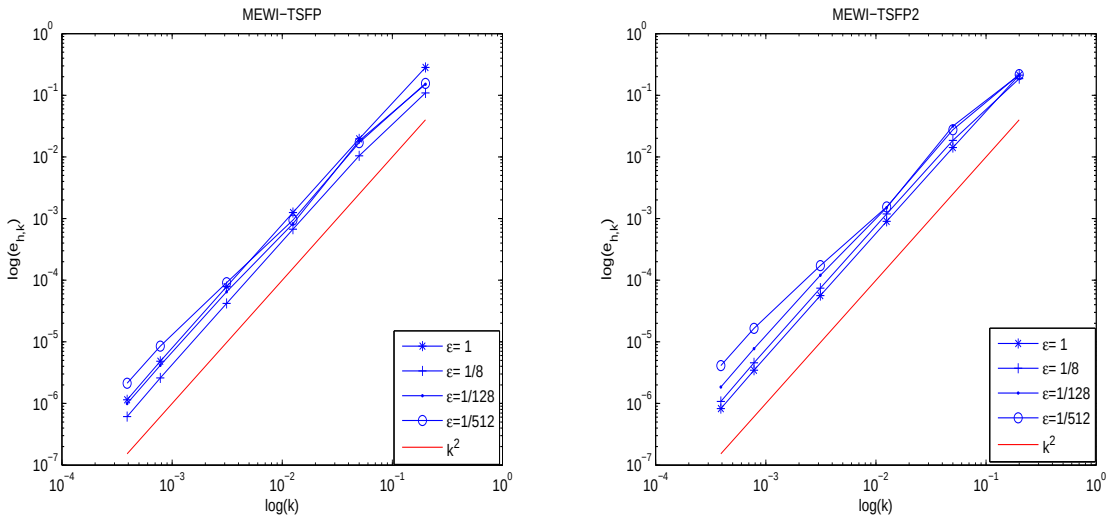

Figure 4.1: Dependence of the temporal errors of EWI-TSFP and EWI-TSFP2 on k at $t = 2$ with different ε for the ill-prepared initial problem.

Table 4.2: Temporal error analysis for $e_{h,k}$ of MEWI-TSFP2 at $T = 2$ with ill-prepared initial data.

MEWI-TSFP2	$k_0 = 0.2$	$k_0/4$	$k_0/2^4$	$k_0/2^6$	$k_0/2^8$	$k_0/2^9$
$\varepsilon_0 = 1$	2.12E-1	1.42E-2	8.99E-4	5.63E-5	3.47E-6	8.24E-7
$\varepsilon_0/2$	2.01E-1	1.35E-2	8.56E-4	5.36E-5	3.30E-6	7.84E-7
$\varepsilon_0/2^2$	1.83E-1	1.18E-2	7.37E-4	4.60E-5	2.83E-6	6.72E-7
$\varepsilon_0/2^3$	1.86E-1	1.85E-2	1.19E-3	7.41E-5	4.56E-6	1.08E-6
$\varepsilon_0/2^4$	2.22E-1	2.14E-2	1.33E-3	8.10E-5	4.94E-6	1.17E-6
$\varepsilon_0/2^5$	1.65E-1	2.41E-2	1.37E-3	7.80E-5	4.71E-6	1.11E-6
$\varepsilon_0/2^6$	2.14E-1	3.15E-2	1.50E-3	1.20E-4	7.76E-6	1.85E-6
$\varepsilon_0/2^7$	2.34E-1	2.14E-2	2.13E-3	1.09E-4	6.87E-6	1.65E-6
$\varepsilon_0/2^8$	2.46E-1	3.51E-2	3.31E-3	1.87E-4	1.29E-5	3.08E-6
$\varepsilon_0/2^9$	2.16E-1	2.75E-2	1.54E-3	1.72E-4	1.65E-5	4.11E-6
$\varepsilon_0/2^{10}$	2.33E-1	3.60E-2	1.74E-3	3.85E-4	2.57E-5	6.60E-6

Table 4.3: Spatial error analysis for $e_{h,k}$ of MIT-TSFP at $T = 2$ with extremely ill-prepared initial data.

MIT-TSFP	$h_0 = 1$	$h_0/2$	$h_0/4$	$h_0/8$
$\varepsilon_0 = 1$	2.06E-1	6.28E-4	2.86E-8	2.51E-11
$\varepsilon_0/2$	1.13E-1	5.27E-4	2.64E-8	1.18E-11
$\varepsilon_0/2^2$	9.25E-2	4.90E-4	2.53E-8	7.06E-12
$\varepsilon_0/2^3$	6.24E-2	5.28E-4	2.47E-8	7.12E-12
$\varepsilon_0/2^4$	6.05E-2	4.39E-4	2.49E-8	1.38E-11
$\varepsilon_0/2^5$	6.00E-2	4.37E-4	2.42E-8	1.39E-11
$\varepsilon_0/2^6$	5.99E-2	4.34E-4	2.42E-8	9.08E-12
$\varepsilon_0/2^7$	5.99E-2	4.34E-4	2.41E-8	6.80E-12
$\varepsilon_0/2^8$	5.99E-2	4.34E-4	2.41E-8	1.39E-11
$\varepsilon_0/2^9$	5.99E-2	4.34E-4	2.40E-8	1.39E-11
$\varepsilon_0/2^{10}$	5.99E-2	4.34E-4	2.40E-8	1.39E-11

Chapter 5

Conclusion remarks and future work

This thesis is devoted to studying the efficient and accurate numerical methods for solving the Klein-Gordon-Schrödinger (KGS) equations in the singular limit regime, i.e. $0 < \varepsilon \ll 1$. In the first part, energy conservative finite difference (ECFD) method, semi-implicit finite difference (SIFD) method and Crank-Nicoson time-splitting Fourier pseudospectral (CNTSFP) method were reviewed as well as compared with each other for solving the KGS equations in the singular limit regime under three types of initial data. The error estimate of ECFD when $\varepsilon = O(1)$ was provided in Chapter 2, which showed the error bound and convergence rate of ECFD from theoretical point of view. Extensive numerical results on the KGS equations with the three types of initial data were reported to demonstrate the efficiency, accuracy and ε-scalability of these methods. Based on the numerical results, we found that all the methods have uniform accuracy in space for solving the different types of initial problems except for the ECFD and SIFD methods, which have $h^2/\sqrt{\varepsilon}$ error bound in space for solving the extremely ill-prepared data problem. All the methods have uniform second-order accuracy in time only for solving the KGS equations with well-prepared initial data when $0 < \varepsilon \ll 1$. The numerical results also show that ECFD, SIFD and CNTSFP have asymptotic temporal error bound $O(k^2/\varepsilon^2)$ for solving the ill-prepared initial data problem and $O(k^2/\varepsilon^3)$ for solving the extremely ill-prepared initial data problem. In addition, all of the methods have

some convergence order reductions or lose the convergence of temporal error outside the convergence regime, which means when ε is very small, these methods are not efficient nor optimal for solving the KGS equations numerically except for taking k sufficiently small.

In the second part of this thesis, we focused on the KGS equations with the ill-prepared and extremely ill-prepared initial data in the singular limit regime, of which the solutions have high oscillation in time with respect to ε. Based on the exponential wave integrator (EWI) method for solving the second order nonlinear ODEs and time-splitting algorithm for the Schrödinger equation, we proposed two uniformly accurate, efficient and explicit methods (EWI-TSFP) for the KGS equations. Numerical studies of these two methods were carried out for the ill-prepared initial and extremely ill-prepared problem, which showed that these two methods have uniform and optimal spectral accuracy in space and they are uniformly accurate in time with quadratic convergence rate when $0 < k \leq \varepsilon$. Compared with the results of the classical methods, the new methods offer better approximations for the KGS equations when $0 < \varepsilon \ll 1$. Two multiscale methods were proposed based on the multiscale analysis of the KGS equations and the applications of EWI-TSFP and EWI-TSFP2 methods for the decomposed KGS with ill-prepared initial data. Numerical results showed that the multiscale methods have uniform spectral accuracy in space and uniform second-order accuracy in time. Thus for solving the KGS equations with the ill-prepared initial data, the multiscale methods are the best with uniform and optimal accuracy compared with other methods we discussed. The limitation of the two multiscale methods is that they can only solve the KGS equations in the singular limit regime with the ill-prepared initial data. Once the type of the initial conditions is changed to other types, new multiscale schemes need to be designed.

To our knowledge, the error estimate of the numerical methods are very difficult to establish because of the two coupling terms in the KGS equations and one small parameter ε. Even for the finite difference method, it has not been done. In the

future work, we will focus on general error estimates for finite difference methods and CNTSFP when $0 < \varepsilon \ll 1$. In addition, we will try to further improve the performance of the uniformly accurate multiscale methods for solving the KGS equations with extremely ill-prepared initial data and establish the theoretical error estimate for the EWI-TSFP method.

Bibliography

[1] S. Ahmed, Solitary waves for Klein-Gordon-Schrödinger equations with perturbed term, Adv. Studies Theor. Phys., 6 (2012), pp. 553-562.

[2] J. B. Baillon and J. M. Chadam, The Cauchy problem for the coupled Schrödinger-Klein-Gordon equations, North-Holland Math. Studies, 30 (1978), pp. 37-44.

[3] A. D. Bandrauk and H. Shen, Exponential split operator methods for solving coupled time-dependent Schrödinger equations, J. Chern. Phys., 99 (1993), pp. 1185-1193.

[4] W. Bao and Y. Cai, Mathematical theory and numerical methods for Bose-Einstein condensation, Kinet. Relat. Mod., 6 (2013), pp. 1-135.

[5] W. Bao and Y. Cai, Uniform error estimates of finite difference methods for the nonlinear Schrödinger equation with wave operator, SIAM J. Numer. Anal., 50 (2012), pp. 492-521.

[6] W. Bao and Y. Cai, Uniform and optimal error estimates of an exponential wave integrator sine pseudospectral method for the nonlinear Schrödinger equation with wave operator, SIAM J. Numer. Anal., 52 (2014), pp. 1103-1127.

[7] W. Bao, Y. Cai, and X. Zhao, Uniformly correct multiscale time integrator pseudospectral method for klein-gordon equation in the non-relativistic limit regime, SIAM J. Numer. Anal., 52 (2014), pp. 2488-2511.

[8] W. Bao and X. Dong, Analysis and comparison of numerical methods for the Klein-Gordon equation in the nonrelativistic limit regime, Numer. Math., 120 (2012), pp. 189-229.

[9] W. Bao, X. Dong, and X. Zhao, An exponential wave integrator pseudospectral method for the Klein-Gordon-Zakharov system, SIAM J. Sci. Comput., 35 (2013), pp. 2903-2927.

[10] W. Bao, X. Dong and S. Wang, Singular limits of Klein-Gordon-Schrödinger equations to Schrödinger-Yukawa equations, Multiscale Model. Simul., 8 (2010), pp. 1742-1769.

[11] W. Bao, D. Jaksch and P. A. Markowich, Numerical solution of the Gross-Pitaevsikii equation for Bose-Einstein condensation, J. Comput. Phys., 187 (2003), pp. 318-342.

[12] W. Bao, S. Jin and P. A. Markowich, Numerical study of time-splitting spectral discretizations of nonlinear Schrödinger equations in the semiclassical regimes, SIAM J. Sci. Comput., 25 (2003), pp. 27-64.

[13] W. Bao and F. F. Sun, Effcient and stable numerical methods for the generalized and vector Zakharov system, SIAM J. Sci. Comput., 26 (2005), pp. 1057-1088.

[14] W. Bao and L. Yang, Efficient and accurate numerical methods for the Klein-Gordon- Schrödinger equations, J. Comput. Phys., 225 (2007), pp. 1863-1893.

[15] C. Bardeen, Feedback quantum control of molecular electronic population transfer, Chem. Phys. Lett., 280 (1997) pp. 151-158.

[16] P. Biler, Attractors for the system of Schrödinger and Klein-Gordon equations with Yukawa coupling, SIAM J. Math. Anal., 21 (1990), pp. 1190-1212.

[17] J. D. Bjorken and S. D. Drell, Relativistic quantum mechanics, McGraw-Hill Book Company, 1964.

[18] P. Brenner and W. von Wahl, Global classical solutions of nonlinear wave equations, Math. Z., 176 (1981), pp. 87-121.

[19] H. Brezis and T. Gallouet, Nonlinear Schrödinger evolution equations, J. Nonlinear Anal., 4 (1980), pp. 677-681.

[20] L. D. Broglie, Nonlinear wave mechanics, Elsevier, Amsterdam, 1960.

[21] J. X. Cai, B. Yang and H. Liang, Multisymplectic implicit and explicit methods for Klein-Gordon-Schrödinger equations, Chin. Phys. B, 22 (2013), 030209.

[22] P. Chartier, N. Crouseilles, M. Lemou and F. Méhats, Uniformly accurate numerical schemes for highly oscillatory Klein-Gordon and nonlinear Schrödinger equations, Numer. Math., 129 (2013), pp. 211-250.

[23] Q. Chang and H. Jiang, A conservative difference scheme for the Zakharov equations. J. Comput. Phys., 113 (1994), pp. 309-319.

[24] A. Darwish and E. G. Fan, A series of new explicit exact solutions for the coupled Klein-Gordon-Schrödinger equations, Chaos, Solitons Fractals, 20 (2004), pp. 609-617.

[25] M. Dehghan, A. Mohebbi and Z. Asghari, Fourth-order compact solution of the nonlinear Klein-Gordon equation, Numer. Algor., 52 (2009), pp. 523-540.

[26] M. Dehghan and A. Ghesmati, Application of the dual reciprocity boundary integral equation technique to solve the nonlinear Klein-Gordon equation, Comput. Phys. Commun., 181 (2010), pp. 1410-1418.

[27] M. Dehghan and A. Shokri, A numerical method for solution of the two-dimensional sine-Gordon equation using the radial basis functions, Math. Comput. Simul., 79 (2008), pp. 700-715.

[28] M. Dehghan, On the solution of an initial-boundary value problem that combines Neumann and integral condition for the wave equation, Numer. Methods Partial Diff. Equat., 21 (2005), pp. 24-40.

[29] M. Dehghan and A. Taleei, Numerical solution of the Yukawa-coupled Klein-Gordon-Schrödinger equations via a Chebyshev pseudospectral multidomain method, Appl. Math. Modelling, 36 (2012), pp. 2340-2349.

[30] J. M. Dixon, J. A. Tuszynski and P. J. Clarkson, From nonlinearity to coherence: universal features of nonlinear behavior in many-body physics, Cambridge University Press, Cambridge, 1997.

[31] W. E, Dynamics of vortices in Ginzburg-Landau theroties with applications to superconductivity, Phys. D, 77 (1994), pp. 38-404.

[32] W. E and B. Engquist, The heterogeneous multiscale methods, Comm. Math. Sci., 1 (2003), pp. 87-132.

[33] E. Fernandez-Cara and E. Zuazua, Control theory: history, mathematical achievement and perspectives, Bol. Soc. Math. Apl., 26 (2003), pp. 79-140.

[34] I. Fukuda and M. Tsutsumi, On the Yukawa-coupled Klein-Gordon-Schrödinger equations in three space dimensions, Proc. Japan Acad., 51 (1975), pp. 402-405.

[35] I. Fukuda and M. Tsutsumi, On coupled Klein-Gordon-Schrödinger equations II, J. Math. Anal. Appl., 66 (1978), pp. 358-378.

[36] I. Fukuda and M. Tsutsumi, On coupled Klein-Gordon-Schrödinger equations III, Math. Japan, 24 (1979), pp. 307-321.

[37] V. Grimm, On error bounds for the Gautschi-type exponential integrator applied to oscillatory second-order differential equations. Numer. Math., 100 (2005), pp. 71-89.

[38] V. Grimm, A note on the Gautschi-type method for oscillatory second-order differential equations, Numer. Math., 102 (2005), pp. 61-66.

[39] B. L. Guo, Global solution for some problem of a class of equations in interaction of complex Schrödinger field and real Klein-Gordon field, Sci. Chin. Ser. A, 25 (1982), pp. 97-107.

[40] B. L. Guo and C. X. Miao, Asymptotic behavior of coupled Klein-Gordon-Schrödinger equations, Sci. Chin. Ser. A, 25 (1995), pp. 705-714.

[41] B. L. Guo and Y. S. Li, Attractor for dissipative Klein-Gordon-Schrödinger equations in R3, J. Diff. Eq., 136 (1997), pp. 356-377.

[42] E. Hairer, C. Lubich and G. Wanner, Geometric numerical integration: structure-preserving algorithms for ordinary differential equations, Springer, Berlin, 2006.

[43] A. Hasegawa and Y. Kodama, Solitons in optical communications, Oxford University Press, New York, 1995.

[44] N. Hayashi and W. von Wahl, On the global strong solutions of coupled Klein-Gordon-Schrödinger equations, J. Math. Soc. Jpn., 39 (1987), pp. 489-497.

[45] E. Hesameddini and F. Fotros, Solution for time-fractional coupled Klein-Gordon-Schrödinger equation using decomposition method, International Math. Forum, 7 (2012), pp. 1047-1056.

[46] J. Hesthaven, S. Gottlieb and D. Gottlieb, Spectral methods for time-dependent problems, Cambridge University Press, Cambridge, 2007.

[47] F. T. Hioe, Periodic solitary waves for two coupled nonlinear Klein-Gordon and Schrödinger equations, J. Phys. A: Math. Gen., 36 (2003), pp. 7307-7330.

[48] M. H. Holmes, Introduction to perturbation methods, Springer Science Business Media (Vol. 20), 2012.

[49] J. Hong, S. Jiang and C. Li, Explicit multi-symplectic methods for Klein-Gordon-Schrödinger equations, J. Comput. Phys. 228 (2009), pp. 3517-3532.

[50] J. Hong, S. Jiang, L. Kong and C. Li, Numerical comparison of five difference schemes for coupled Klein-Gordon-Schrödinger equations in quantum physics, J. Phys. A: Math. Theor., 40 (2007), pp. 9125-9135.

[51] W. Jia, L. Biao and Y. Wang, Approximate solution for the Klein-Gordon-Schrödinger equation by the homotopy analysis method, Chin. Phys. B, 19 (2010), pp. 300-401.

[52] N. I. Karachalios, N. M. Stavrakakis and P. Xanthopoulos, Parametric exponential energy decay for dissipative electron-ion plasma waves, Z. Angew. Math. Phys., 56 (2005), pp. 218-238.

[53] K. R. Khusnutdinova, Coupled Klein-Gordon equations and energy exchange in two-component systems, Eur. Phys. J. Special Topics, 147 (2007), pp. 45-72.

[54] L. Kong, J. Hong and R. Liu, Long-term numerical simulation of the interaction between a neutron field and a neutral meson field by a symplecticpreserving scheme, J. Phys. A, 41 (2008), pp. 207-255.

[55] L. Kong, R. Liu and Z. Xu, Numerical simulation of interaction between Schrödinger field and Klein-Gordon field by multisymplectic method, Appl. Math. Comput., 181 (2006), pp. 342-350.

[56] L. Kong, J. Zhang, Y. Cao, Y. Duan and H. Huang, Semi-explicit symplectic partitioned Runge-Kutta Fourier pseudospectral scheme for Klein-Gordon-Schrödinger equations, Comput. Phys. Commun., 181 (2010) pp. 1369-1377.

[57] Y. Li and B. Guo, Asymptotic smoothing effect of solutions to weakly dissiptive Klein-Gordon-Schrödinger equations, J. Math. Annl. Appl., 282 (2003), pp. 256-265.

[58] H. Liang, Linearly implicit conservative schemes for long-term numerical simulation of Klein-Gordon-Schrödinger equations, Appl. Math. and Comput., 238(2014), pp. 475-484.

[59] K. N. Lu and B. X. Wang, Global attractors for the Klein-Gordon-Schrödinger equation in unbounded domains, J. Diff. Eq., 170 (2001), pp. 281-316.

[60] V. G. Makhankov, Dynamics of classical solitons (in non-integrable systems), Phys. Lett. C, 35 (1978), pp. 1-128.

[61] F. Natali and A. Pastor, Stability properties of periodic standing waves for the Klein-Gordon-Schrödinger system, Commun. Pure Appl. Anal., 9 (2010), pp. 413-430.

[62] M. Ohta, Stability of stationary states for the coupled Klein-Gordon-Schrödinger equations, Non. Anal., 27 (1996), pp. 455-461.

[63] T. Ozawa and Y. Tsutsumi, Asymptotic behaviour of solutions for the coupled Klein-Gordon-Schrödinger equations, Adv. Stud. Pure Math., 23 (1994), pp. 295-305.

[64] T. Ozawa and Y. Tsutsumi, The nonlinear Schrödinger limit and the initial layer of the Zakharov equations, Diff. Int. Eqs., 5 (1992), pp. 721-745.

[65] A. P. Peirce, M. A. Dahleh and H. Rabitz, Optimal control of quantum mechanical systems: existence, numerical approximation and applications, Phys. Rev. A, 37 (1988), pp. 4950-4964.

[66] V. Petviashvili and O. Pokhotelov, Solitary waves in plasmas and in the atmosphere, Gordon and Breach, Philadelphia, 1992.

[67] S. Ray, An application of the modified decomposition method for the solution of the coupled Klein-Gordon-Schrödinger equation, Commun. Nonlinear Sci. Numer. Simul., 13 (2008), pp. 1311-1317.

[68] J. J. Sakurai, Advanced quantum mechanics, Addison-Wesley, 1967.

[69] A. W. Schreiber and R. Rosenfelder, First-order variational calculation of form factor in a scalar nucleon-meson theory, Nucl. Phys. A, 601 (1996), pp. 397-424.

[70] F. Shakeri and M. Dehghan, Numerical solution of the KleinGordon equation via He's variational iteration method, Nonlinear Dynam., 51 (2008), pp. 89-97.

[71] Y. R. Shen, Principles of nonlinear optics, Wiley, New York, 1984.

[72] C. Sulem and P. L. Sulem, The nonlinear Schrödinger equation: self-focusing and wave collapse, Springer, Berlin, 1999.

[73] X. Y. Tang and W. Ding, The general Klein-Gordon-Schrödinger system: modulational instability and exact solutions, Phys. Scr., 77 (2008), 015004.

[74] K. Veselic, On the nonrelativistic limit of the bound states of the Klein-Gordon equation, J. Math. Anal. Appl., 96 (1983), pp. 63-84.

[75] W. von Wahl, Analytische Abbildungena nd semilineare Diffe rentialgleichungeni n Banachräumen, Nachr. Akad. Wiss. Göttingen II : Math.-Phys. Kl., (1979), pp. 153- 200.

[76] W. von Wahl, Nichtlineare Evolutionsgleichungen, Teubner Texte zur Math., 50 (1983), pp. 294-302.

[77] W. von Wahl, Über das Verhalten für $t \to 0$ der Lösungen nichtlinearer parabolischer Gleichungen, insbesondere der Gleichungen von Navier-Stokes, Bayreuth. Math. Schr., 16 (1984), pp. 151-277.

[78] M. L. Wang and Y. B. Zhou, The periodic wave solutions for the Klein-Gordon-Schrödinger equations, Phys. Lett. A, 318 (2003), pp. 84-92.

[79] Q. Wang, Theoretical issue of controlling nucleus in Klein-Gordon-Schrödinger dynamics with perturbation in control field, Appl. Math. Comput., 206 (2008), pp. 276-289.

[80] S. Wang and L. Zhang, A class of conservative orthogonal spline collocation schemes for solving coupled Klein-Gordon-Schrödinger equations, Appl. Math. Comput., 203 (2008), pp. 799-812.

[81] T. Wang and Y. Jiang, Point-wise errors of two conservative difference schemes for the Klein-Gordon-Schrödinger equation, Commun. Nonlinear Sci. Numer. Simulat., 17 (2012), pp. 4565-4575.

[82] T. Wang, Optimal point-wise error estimate of a compact difference scheme for the Klein-Gordon-Schrödinger equation, J. Math. Anal. Appl., 412 (2014), pp. 155-167.

[83] Y. H. Wang and B. Wang, High-order multi-symplectic schemes for the nonlinear Klein-Gordon equation, Appl. Math. Comput., 166 (2005), pp. 608-632.

[84] Y. P. Wang and D. F. Xia, Generalized solitary wave solutions for the Klein-Gordon-Schrödinger equations, Comput. Math. Appl., 58 (2009), pp. 2300-2306.

[85] R. A. Weder, Scattering theory for the Klein-Gordon equation, J. Func. Anal., 27 (1978), pp. 100-117.

[86] S. Weinberg, The quantum theory of fields, Cambridge University Press, 1995.

[87] P. Xanthopoulos and G. Zouraris, A linearly explicit finite different method for a Klein-Gordon-Schrödinger system modeling electron-ion plasma waves, Discrete Contin. Dyn. Syst. Ser. B, 10 (2008), pp. 239-263.

[88] J. Xia, S. Han and M. Wang, The exact solitary wave solution for the Klein-Gordon-Schrödinger equations, Appl. Math. Mech., 23 (2002), pp. 52-58.

[89] X. M. Xiang, Spectral method for solving the system of equations of Schrödinger-Klein-Gordon field, J. Comput. Appl. Math., 21 (1988), pp. 161-171.

[90] E. Yomba, On exact solutions of the coupled Klein-Gordon-Schröodinger and the complex coupled KdV equations using mapping method, Chaos, Solitons and Fractals, 21 (2004), pp. 209-229.

[91] H. Yukawa, On the interaction of elementary particles, I , Proc. Phys. Math. Soc. Japan, 17 (1935), pp. 48-57.

[92] V. E. Zakharov, Collapse of Langmuir waves, Sov. Phys. JETP, 35 (1972), pp. 908-912.

[93] L. M. Zhang, Convergence of a conservative difference scheme for a class of Klein-Gordon-Schrödinger equations in one space dimension, Appl. Math. Comput., 163 (2005), pp. 343-355.

Numerical Studies on the Klein-Gordon-Schrödinger equations in the Singular Limit Regime **Hong Mei** **2015**